GRAPE Working Paper #101

Demographic transition and the rise of wealth inequality

Krzysztof Makarski, Joanna Tyrowicz, and Piotr Żoch

FAME | GRAPE, 2025

Foundation of Admirers and Mavens of Economics
Group for Research in Applied Economics

Demographic transition and the rise of wealth inequality

Krzysztof Makarski
FAME|GRAPE and SGH

Joanna Tyrowicz
FAME|GRAPE,
University of
Augsburg, and IZA

Piotr Żoch
FAME|GRAPE,
and University of Warsaw

Abstract

We analyze the contribution of rising longevity to the increase in wealth inequality in the U.S. over the past seventy years. To do so, we construct an overlapping generations (OLG) model with multiple sources of inequality, carefully calibrated to the data. Our key finding is that improvements in old-age longevity have a substantial impact on wealth inequality, accounting for approximately half the effect of income inequality, which has been the focus of much of the existing literature. In contrast, the impact of tax changes is relatively minor. The contribution of rising longevity is expected to continue driving wealth inequality upward in the coming decades.

Keywords:

wealth inequality, rising longevity, OLG

JEL Classification

J15, D31, E21, E24

Corresponding author

Piotr Żoch, p.zoch@uw.edu.pl

Acknowledgements

We thank Roel Beetsma, Fabian Kindermann, Per Krusell, Iga Magda, Ward Romp, and Nancy Stokey for their valuable discussions and insights. We are especially grateful to Piotr Dworczak and Oliwia Komada for their thoughtful comments and suggestions. We also wish to acknowledge the Editor, Francesco Lippi, and four anonymous referees, whose constructive feedback greatly enhanced this paper. Additionally, we appreciate the comments revived from the participants of AEA 2022, CEF 2022, and IIPF 2022. We are indebted to Marcin Lewandowski for his excellent research assistance. This project was supported by National Science Center (grant \#2016/22/E/HS4/00129) whose generosity is greatly appreciated. Any remaining errors are entirely our own.

Published by: FAME | GRAPE
ISSN: 2544-2473

Foundation of Admirers and Mavens of Economics
Koszykowa 59/7
00-660 Warszawa
Poland

W | grape.org.pl
E | grape@grape.org.pl
TT | GRAPE_ORG
FB | GRAPE.ORG
PH | +48 799 012 202

1 Introduction

We study the role of longevity and rising income inequality in the growth of wealth inequality in the United States. A large body of literature documents a rise in income inequality (e.g. Chetty et al., 2017; Guvenen et al., 2022) and attributes growing wealth inequality in the U.S. to rising income inequality (e.g. Saez and Zucman, 2016; Piketty et al., 2018). Hubmer et al. (2021) argue that continuing with the 1970s redistribution in the tax system into the next decades could have prevented the rise in wealth inequality even in the presence of high income inequality.

At the same time, the U.S. experienced a colossal increase in life expectancy, especially in old-age longevity. Between 1970 and 2015, life expectancy at 65 has improved from slightly above 14 years to nearly 19 years. Through the lens of any standard overlapping generations model, this rise in longevity can translate to an increase in wealth inequality due to two mechanisms. First, since individuals expect to live longer, a behavioral effect involves higher wealth accumulation at the peak of the life cycle for each subsequent birth cohort.Second, a composition effect appears due to a rising share of individuals close to the peak of wealth accumulation. In this paper, we quantify the role of demographics in rising wealth inequality and juxtapose it with income inequality.

The two drivers of wealth inequality – longevity and income inequality – yield markedly different policy recommendations. If driven by longevity, the rise in wealth inequality merely indicates that households internalize the changing demographic trends in their lifetime optimization. If caused by the rise of income inequality, it has a number of implications (such as an amplification of labor market processes to old age poverty) that necessitate policy interventions. Hence, emerges policy relevance of our study.

Our main contribution is demonstrating that demographic factors significantly influence wealth inequality. We build a general equilibrium overlapping generations model that replicates key trends in the data, including a decline in the wealth Gini coefficient until the late 1970s, followed by a 5-point increase. Individuals in the model are ex-ante heterogeneous, differing by education, which affects their mortality risk and labor income. They face uncertainty throughout life due to income risk, discount rate shocks, and risky returns on savings.

The model is carefully calibrated to U.S. data. It replicates the 1930s economy as the initial steady state and tracks wealth inequality dynamics during the transition to a new steady state. We model changes in longevity using survival probabilities aligned with demographic data and projections. We allow for multiple sources of changes in the income distribution: time-varying shares of college-educated individuals, skill premia, and evolving income risk for subsequent cohorts. Redistribution mechanisms consistent with the data, including varying tax rates and income tax progressivity, are also incorporated.

We use this model to perform counterfactual simulations by setting mortality risk, income mechanisms, and taxes to their 1950s levels. We show that the impact of longevity is quantitatively substantial, with the size of the effect roughly half as large as that of the observed changes in income inequality. Our findings also reveal that the behavioral channel, driven by consumption-savings responses to longer lifespans, plays a larger role than changes in demographic structure. In contrast, the contribution of the tax system is relatively minor. Finally, using demographic projections, we examine the future trajectory of wealth inequality and find that current forces will continue to amplify inequality for another half-century.

The related literature We build on a rich tradition of quantitative macroeconomic models (originating from Bewley, 1977). The early models faced challenges in replicating the degree of wealth

inequality observed in the data, even after accounting for idiosyncratic income shocks.[1] Since then, the literature has branched into three strands reflecting the role of different forms of heterogeneity in shaping wealth inequality: (i) heterogeneous incomes, (ii) heterogeneous savings, and (iii) heterogeneous returns on assets.

For heterogeneous incomes, particularly the thickness of the upper tail plays a central role. Castaneda et al. (2003); Benhabib et al. (2019); Gabaix et al. (2016) demonstrate that persistent and skewed earnings processes (also known as "superstars") generate wealth distributions that resemble empirical patterns. Taxing "super-luck" improves welfare and optimal taxation of "superstars" reduces wealth concentration due to reduced income concentration (Kindermann and Krueger, 2022). An alternative approach shows that even if the increase in income inequality is transitory, the effects on wealth inequality are partially persistent (Lippi and Perri, 2023). Kaymak and Poschke (2016) attribute over half of the post-1960 rise in U.S. wealth inequality to increasing earnings inequality. Redistribution through taxation plays an important role as well. The decline in redistribution can explain the evolution of the top income shares (Aoki and Nirei, 2017) and wealth inequality (Hubmer et al., 2021).

Another important mechanism is the heterogeneity in savings rates. Higher savings rates are observed among the wealthy (Straub, 2019).[2] De Nardi (2004) and Cagetti and De Nardi (2006) show that the variation of bequests is instrumental in replicating key features of observed wealth distributions.

For heterogeneity of returns on assets, the literature offers two distinct channels. First, a strand of research shows that rates of return generally increase with wealth (see Kuhn et al., 2020; Hubmer et al., 2021). Second, the literature emphasizes the theoretical and quantitative role of the dispersion of the returns (see Benhabib et al., 2011, 2019; Fagereng et al., 2020; Bach et al., 2020; Gomez, 2024). Gomez and Gouin-Bonenfant (2024) integrate both of these channels, demonstrating that they jointly contribute to increasing inequality at the top of the wealth distribution.

The role of demographics is increasingly being recognized in macroeconomic models.[3] However, the role of demographics in wealth inequality is largely unexplored. Krueger and Ludwig (2007) use an OLG model to compare wealth inequality in the U.S., EU, and OECD under different longevity and immigration scenarios but do not isolate the effect of rising longevity. Many other studies on wealth inequality rely on infinitely lived agent models (e.g. Aoki and Nirei, 2017; Hubmer et al., 2021),[4] or focus on steady states and simulate transition paths for policies (e.g. Kindermann and Krueger, 2022). To the best of our knowledge, this is the first study to systematically quantify the role of rising longevity in explaining the dynamics of wealth inequality.

In comparison to the existing literature, our paper offers several novelties. First, we focus explicitly on the effects of rising longevity on wealth inequality. Using a rich OLG model carefully calibrated to data, we replicate the observed dynamics of wealth inequality, which allows us to isolate the role of demographics by removing time variation in selected model inputs. Second, we account for multiple

[1] For example, Aiyagari (1994) calibrated his model to match PSID data and produced a wealth Gini coefficient of 40, that is roughly a half the empirical estimate of 80.

[2] Empirical evidence is mixed: Fagereng et al. (2019) show that *net* savings rates are relatively constant across the wealth distribution in Norway. Behavioral heterogeneity was used to replicate savings rate heterogeneity in structural models. The extensive literature explores heterogeneity in preferences (e.g. Epper et al., 2020) as well as financial literacy (e.g. Lusardi et al., 2017).

[3] The demographic transition has been a key driver of the decline in observed (Eggertsson et al., 2019) and natural (Bielecki et al., 2020) interest rates in the recent decades. In a deterministic OLG setup, Gagnon et al. (2021) demonstrate that demographics contributed to permanent declines in real GDP growth, aggregate investment rates, and safe asset yields in the US. In a stochastic OLG setup, Auclert et al. (2021) predict that aging will raise wealth-to-GDP ratios, lower asset returns, and exacerbate global imbalances.

[4] Kaymak and Poschke (2016) use a simplified two-stage life cycle model with working and retirement phases.

potential channels of spillover from income inequality to wealth inequality. Our model incorporates numerous sources of idiosyncratic shocks. We can thus compare the strength of demographics with other channels, such as income inequality and taxation. Last but not least, we study wealth inequality for the "bottom 99%".[5] In fact, the rise of wealth inequality irrespective of the wealthiest percentile of the population was large and demographic factors have played an important role in this process. Demographics likely have less impact on top wealth inequality. Given the focus of our study, our aim is to analyze the broader wealth distribution rather than its extremes. For this reason, we use the Gini coefficient as our primary measure of wealth inequality.

2 Model

We construct a general equilibrium OLG model with heterogeneous households. Agents have perfect foresight with respect to aggregate variables. We describe the household sector below. The rest of the model is relegated to the Online Appendix A.

2.1 Population dynamics

Households are finitely lived, their age is denoted by $j \in \{1, \ldots, J\}$. Let $s \in \{L, H\}$ be the level of education of a household, with $s = L$ being less than college, and $s = H$ being some college education or more. The size of the cohort j in period t with educational level s is $N_{j,t,s}$ and $N_{j,t}$ denotes the total size of the population of age j at time t. The size of each new cohort $N_{1,t}$ and the fractions by education status s are determined exogenously. The s-specific conditional probability of survival from age j to $j+1$ in period t is $\psi_{s,j,t}$. Finally, the total population is $N_t = \sum_{j=1}^{J} N_{j,t}$.

The size of cohort j in period t is $N_{j,t} = \sum_{s \in \{L,H\}} N_{s,j,t}$, with $N_{s,j,t}$ denoting the size of population with education level s of age j at time t. The size of each new cohort of education s, $N_{s,1,t}$, is determined exogenously. Given education level, specific conditional probability of survival from age j to age $j+1$ in period t is $\psi_{s,j,t}$ the population evolves according to $N_{s,j+1,t+1} = \psi_{s,j,t} N_{s,j,t}$.

2.2 Budget constraint

Let $\bar{j}$ denote the retirement age. Households with $j < \bar{j}$ face the wage rate $w_t e_{s,j,t}$, where w_t denotes wage per unit of efficiency labor (marginal product of aggregate labor), $e_{s,j,t}$ represents idiosyncratic wage variation due to the education level s, age j, and a random component ω which follows a first-order Markov chain with states $\omega_{s,j,t}$ and transition matrix $\pi^{\omega}_{s,j,t}(\omega_{s,j+1,t+1} \mid \omega_{s,j,t})$.[6] The details of the $e_{s,j,t}$ are discussed later in conjunction with equation (3). Households with $j \geq \bar{j}$ have $e_{s,j,t} = 0$.

Labor income of a working household is subject to a social security contribution at the rate $\tau_{ss,t}$. The base of the labor income tax is thus $y_{s,j,t} = (1 - \tau_{ss,t}) w_t e_{s,j,t} \ell_{s,j,t}$, where $\ell_{s,j,t}$ is the labor supply. Households pay progressive labor income tax $\mathcal{T}_t(y_{s,j,t}, \bar{y}_t)$ given by $\mathcal{T}_t(y_{s,j,t}, \bar{y}_t) = y_{s,j,t} - (1 - \tau_{\ell,t}) \left(\frac{y_{s,j,t}}{\bar{y}_t}\right)^{1-\lambda_t} \bar{y}_t$, where the elasticity of after-tax to pre-tax income equals $1 - \lambda_t$, and $\tau_{\ell,t}$ determines the average tax rate. The average labor income tax base in period t is denoted by $\bar{y}_t$.[7]

Let $a_{s,j,t}$ denote the holdings of assets at the beginning of the period t. Asset markets are incomplete, households can only self-insure against fluctuations in idiosyncratic labor productivity by

[5] An interesting evidence on wealth inequality dynamics from the *Forbes* 400 list, is provided by Gomez (2023).

[6] Note that states and the transition matrix depend on the education level s, age j, and time period t.

[7] The after-tax labor income can be thus expressed as a weighted geometric mean $(1 - \tau_{\ell,t}) y_{s,j,t}^{1-\lambda_t} \bar{y}_t^{\lambda_t}$.

saving in a risky asset that pays a gross after-tax return $1+\tilde{r}_t+\epsilon^r_{s,j,t}$, where $\tilde{r}_t$ is a deterministic aggregate component and $\epsilon^r_{s,j,t}$ is an i.i.d. idiosyncratic return shock, $\epsilon^r_{s,j,t} \sim N\left(0,\sigma_r^2\right)$. Assets holdings are subject to a borrowing constraint, $a_{s,j+1,t+1} \geq 0$.

Households' resources consist of after-tax labor income $y_{s,j,t}-\mathcal{T}_t\left(y_{s,j,t},\bar{y}_t\right)$, current wealth along with the interest accrued $\left(1+\tilde{r}_t+\epsilon^r_{s,j,t}\right)a_{s,j,t}$, pension benefits $b_{s,j,t}$ (described in Appendix A), and of accidental bequests $\Gamma_{s,j,t}$. The bequests are evenly distributed between all the surviving households of the same education level within a birth cohort. Households use these resources to purchase consumption goods $c_{s,j,t}$ and accumulate wealth, and $\tau_{c,t}$ denotes the consumption tax rate. The budget constraint is thus:

$$a_{s,j+1,t+1}+\left(1+\tau_{c,t}\right)c_{s,j,t}=y_{s,j,t}-\mathcal{T}_t\left(y_{s,j,t},\bar{y}_t\right)+\left(1+\tilde{r}_t+\epsilon^r_{s,j,t}\right)a_{s,j,t}+b_{s,j,t}+\Gamma_{s,j,t}. \quad (1)$$

2.3 Social security

We replicate the main features of the current U.S. pension system: the average index of monthly wages accumulation (AIME) and the cap imposed by Old Age, Survivors, and Disability Insurance (OASDI). Old age benefits $b_{s,j,t}$ at retirement age $\bar{j}$ depend on the replacement rate $p_{\bar{j},t}$, benefit drawing rights $f_{s,\bar{j},t}$ which reflect AIME accumulation, and average earnings in the economy $\overline{w_t e_t \ell_t}$. A time-varying scaling factor $\varrho_{\bar{j},t}$ adjusts the generosity of benefits to maintain a data-consistent ratio of benefits to GDP. The detailed formulae $b_{s,j,t}$, $p_{\bar{j},t}$ and $f_{s,\bar{j},t}$ as well as rationale for $\varrho_{\bar{j},t}$ are relegated to the Online Appendix A.1

2.4 Household problem

Households discount future with $\delta_{s,j,t}$, which follows a first-order Markov chain, and the conditional survival probability $\psi_{s,j,t}$. The individual state variables $z_{s,j,t}$ of the household with education level s and age j in period t are: the level of assets $a_{s,j,t}$, the pension entitlements $f_{s,j,t}$, the level of individual labor productivity $\omega_{s,j,t}$, the level of individual discount factor $\delta_{s,j,t}$, and the rate of return shock $\epsilon^r_{s,j,t}$; $z_{s,j,t}=\left(a_{s,j,t},f_{s,j,t},\omega_{s,j,t},\delta_{s,j,t},\epsilon^r_{s,j,t}\right)\in\Omega$. We assume that households of age $j=1$ enter with no assets, $a_{s,1,t}=0$.

The optimization problem of the household in a recursive form is:

$$\begin{aligned} V_{s,j,t}\left(z_{s,j,t}\right) \;=\; & \max_{\left(c_{s,j,t},\ell_{s,j,t},f_{s,j+1,t+1},a_{s,j+1,t+1}\right)} \frac{1}{1-\theta}\left[c^{\phi}_{s,j,t}\left(1-\ell_{s,j,t}\right)^{1-\phi}\right]^{1-\theta} \\ & +\psi_{s,j,t}\delta_{s,j,t}E\left[V_{s,j+1,t+1}\left(z_{s,j+1,t+1}\right)|z_{s,j,t}\right], \end{aligned} \quad (2)$$

subject to the budget constraint in equation (1), formulas for pensions in equations (A.1) and (A.2), and the borrowing constraint $a_{s,j+1,t+1}\geq 0$, with θ and ϕ determining relative risk aversion and leisure preference, respectively.

2.5 Production function

A representative firm uses capital K_t and labor L_t to produce final output Y_t according to a Cobb-Douglas production function $Y_t=K_t^{\alpha_t}\left(A_tL_t\right)^{1-\alpha_t}$, with labor augmenting technological progress $A_{t+1}/A_t=1+\gamma^A_{t+1}$. Note that both capital income share in total output α_t and the depreciation rate of capital d_t are time varying. Since our production sector is standard, we relegate the description to the Online Appendix A.2.

2.6 Government and Model Closure

Additionally, our model features the government that collects capital income taxes $\tau_{k,t}$, labor income taxes $\mathcal{T}_t(y_{s,j,t}(z_{s,j,t}), \bar{y}_t)$, and consumption taxes $\tau_{c,t}$. The total taxes collected T_t are used to finance government expenditures G_t and subsidize the social security system, with the subsidy being denoted as $\mathcal{S}_t$. Thus, $G_t + \mathcal{S}_t = T_t$. More details on government and market clearing conditions with the definition of equilibrium are relegated to the Online Appendices A.3 and A.4, respectively.

3 Calibration

One period in the model corresponds to five years. In all experiments, we study the transition from the initial steady state in the year 1935 to the final steady state in the distant future. The model is calibrated to match *dynamic features* of the U.S. economy. This implies that many model parameters vary along the transition path, in line with the evolution of real world analogs. Whenever available, we rely on observational data or publicly available forecasts. In a few cases, parametrization of the early years of our model requires extrapolation of the time series to the past and in all instances we also extrapolate the trends in the data to the future years, to obtain a sufficiently distant final steady state for simulations. Below we describe the data sources and target values (if constant). The details for extrapolating the observational data are discussed in Online Appendix B.

3.1 Demographics

We use population data from the Centers for Disease Control and Prevention (CDC). The five-year averages for births and survival probabilities are provided by the United Nations Population database. This data covers historical births and survival probabilities as well as provides a demographic forecast until 2100. We assume that after that year the birth rate continues at 0.06% per year, and survival probabilities stabilize at their 2100 levels.

We calculate the share of households with at least some college ($s = H$ in our model) for each entry cohort using the individual level data from the U.S. Census and American Community Survey. The path of these shares in the data, which we use as inputs for our model, is shown in Figure B.1 of Online Appendix B.1. The survival probabilities in the model, $\psi_{s,j,t}$, depend on the level of education. To capture this heterogeneity, we use U.S. death certificate data from Case and Deaton (2021) that include survival probabilities by cohort, age, and college attainment. The details of processing the data as well as an extrapolation to the periods not covered by the data are described in Online Appendix B.1.

3.2 Income dynamics

We assume an idiosyncratic component of wages, $e_{s,j,t}$, is given by

$$\ln e_{s,j,t} = \beta_{s,t} + \zeta_{s,j} + \omega_{s,j,t}, \tag{3}$$

where $\beta_{s,t}$ is a time-varying component common to all households with the same education level s (college premium), $\zeta_{s,j}$ is a type-specific deterministic age profile and $\omega_{s,j,t}$ follows a first-order Markov chain with states $\omega_{s,j,t}$ and transition matrix $\pi^{\omega}_{s,j,t}\left(\omega_{s,j+1,t+1} \mid \omega_{s,j,t}\right)$.

We normalize $\beta_{L,t} = 1$ and use the (log) college wage premium series from Autor et al. (2020) to construct our measure of $\beta_{H,t}$ and assume it constant after 2020 (see Figure B.3). We estimate the parameters of income processes using the 1970-2019 waves of the Panel Study of Income Dynamics

(PSID). We apply Deaton and Paxson (2000) decomposition to obtain deterministic age profiles $\zeta_{s,j}$, adjusting for cohort and time effects (see Online Appendix B.2.3). We use residuals from this decomposition to estimate a first-order auto-regressive income process:

$$\omega' = \varrho_{\omega,s}\omega + \epsilon_\omega, \quad \epsilon_\omega \sim N\left(0, \sigma^2_{\omega,s,j,t}\right). \tag{4}$$

We allow for different auto-correlation parameters $\varrho_{\omega,s}$ for $s \in \{L, H\}$ and for cohort-specific variances $\sigma^2_{\omega,s,j,t}$. The point estimates are $\varrho_{\omega,L} = 0.980$ and $\varrho_{\omega,H} = 0.985$. We show our estimates of variances in Figure B.5. We adjust estimates of $\varrho_{\omega,s}, \sigma^2_{\omega,s,j,t}$ to reflect the fact that one period in the model corresponds to five years and to have the unconditional expected value $E\left[\exp(\omega)\right] = 1$ for all cohorts. We then approximate each resulting AR(1) process with a 5-state Markov chain by the Rouwenhorst method.

We augment the 5-state Markov chains with an additional 6th state to account for "superstars". This state can be reached only from the 5th state and upon exiting it the household moves to the 3rd state (corresponding to the average productivity for its education level). We calibrate the probability of moving to and falling from the 6th state to match the share of "superstars" in the PSID data, see Online Appendix B.2.3.

3.3 Idiosyncratic returns

Returns on assets in our model consist of two parts: a common aggregate component $\tilde{r}_t$ determined by the marginal product of capital and taxes, and an i.i.d. component $\epsilon_{s,r,t}$ with mean zero. To calibrate the standard deviation of $\epsilon^r_{s,j,t}$, we follow Hubmer et al. (2021). They consider four classes of assets: a risk-free asset, public equity, private equity, and housing, and calculate standard deviation of annual returns by asset class and wealth group (percentiles of wealth distribution). Next, they adopt portfolio weights on these four classes of assets by wealth group from Bach et al. (2020). This allows them to calculate standard deviation of returns on assets by wealth group, $\sigma_{r,\text{group}}$. We take their numbers and calculate average shares of aggregate wealth held by these wealth groups between 1989 and 2022, ϖ_{group}. We provide more details in Online Appendix B.3. The variance of five-year returns in our model is thus $\sigma^2_r = 5\sum_{\text{group}} \varpi^2_{\text{group}} \cdot \sigma^2_{r,\text{group}}$. The implied standard deviation σ_r is 0.123.

3.4 Macroeconomic parameters

Production function We use Penn World Tables 10, published by the Groningen Growth and Development Center (GGDC), to calibrate all the time-varying parameters of the production function. The data for depreciation were adjusted to five-year periods. We set α_t to match labor share in the U.S. in 1950-2019. Labor-augmenting technological progress taken from GGDC is adjusted for time-varying labor share as well as for the changing composition of the labor force (increased share of individuals with $s = H$). The details of processing data and extrapolation are relegated to Online Appendix B.4.

The government Tax rates are calibrated using Mendoza et al. (1994) approach. The rates which match the shares of revenues from capital income tax, labor income tax, and consumption tax observed in the data are obtained from McDaniel (2007). To calibrate labor income tax progressivity, we follow Barro and Sahasakul (1983) and Mertens and Montiel Olea (2018). The government expenditures are determined as a residual to satisfy the government budget constraint. The details are reported in Online Appendix B.5.

Social security To set the effective rate of social security contribution $\tau_{ss,t}$ we use data on social security contributions relative to GDP from the OECD. $\tau_{ss,t}$ determines the ratio of social security contributions to labor income, and the ratio of labor income to GDP (labor share) is pinned down by $1-\alpha_t$. We set retirement age $\bar{j}=10$ to reflect the effective retirement age of 66. The parameters used to calculate pensions in the social security system are taken from McGrattan and Prescott (2017) and remain constant over time. We set parameters controlling the replacement rate $p_{\bar{J},t}$ to match the ratio of pensions to GDP. The details are provided in Online Appendix B.6.

3.5 Preferences

We calibrate the preference for consumption parameter ϕ to match the observed share of hours worked in the economy, which is 33% on average. The relative risk aversion θ is set to 1.5 (in line with Hubmer et al., 2021; Kindermann and Krueger, 2022). The discount factor $\delta_{s,j,t}$ follows a first-order Markov chain with four states. States 1 to 3 and transition probabilities between them are obtained by discretization of an AR(1) process

$$\delta' = (1-\varrho_\delta)\,\bar{\delta} + \varrho_\delta \delta + \epsilon_\delta, \quad \epsilon_\delta \sim N\left(0, \sigma_\delta^2\right),$$

with auto-correlation $\varrho_\delta = 0.992^5$ and standard deviation $\sigma_\delta = 0.006^5$ corresponding to values reported in Hubmer et al. (2021).[8] The fourth state is $\delta_{s,j,t}=0$ and the probability of moving to it from any state is 0.05, calibrated to match the share of hand-to-mouth agents in the data.[9] Once in this state, agents draw $\delta_{s,j,t}$ from its stationary distribution. This means that they can stay in this state for consecutive periods. Similarly, agents with $j=1$ draw $\delta_{s,j,t}$ from the stationary distribution. We set $\bar{\delta}$ to match the pre-tax rate of return on capital of 8% in the initial steady state. The resulting value is 1.01.

4 Model data fit

We begin by evaluating the ability of our model to replicate observed trends in wealth inequality. Our primary focus is on the impact of demographic factors. Since these factors are unlikely to significantly affect the wealth share of the top 1%, we rely on the Gini coefficient as our inequality measure. Figure 1 demonstrates the comparison of model simulations with the data. It shows changes in the Gini coefficient over time, normalized to 1950. The bars represent observed changes from the data, while the solid line reflects the corresponding model simulations.

[8] Discount factor shocks serve as a mechanism to introduce heterogeneity in old-age saving behavior, functioning similarly to a "warm glow" bequest motive or health shocks. The value of ϱ_δ implies that, on average, half of the gap between δ and $\bar{\delta}$ closes within one generation. This level of persistence mimics a structure where altruism is present, with parents caring about the utility of their children. We deliberately chose not to calibrate σ_δ to exactly match the wealth Gini observed in the data, opting instead for the value reported by Hubmer et al. (2021). One reason for this choice is our focus on the "bottom 99%" of the wealth distribution, as we believe demographic processes are less relevant for the top 1%. Using discount factor shocks to match the wealth Gini exactly would risk overemphasizing a factor that may not fully reflect real-world dynamics. This consideration is especially important because our model excludes certain features—such as entrepreneurship or intergenerational transfers—that are recognized in the literature as important for explaining wealth inequality. On the other hand, excluding discount factor shocks entirely would leave the model with fewer sources of inequality, potentially exaggerating the role of demographics. A sensitivity analysis in Online Appendix F.3 confirms this conjecture.

[9] Zeldes (1989) reports that the share of hand-to-mouth agents (households with sufficiently low net worth) was approximately 29% in the earlier waves of the PSID, while Aguiar et al. (2024) reports a share of 23.3% in more recent waves. In our model, the target is an average share of agents aged 25–64 with zero assets, set at 27.5% over the period 1980–2020.

Figure 1: Evolution of wealth inequality: model vs. data

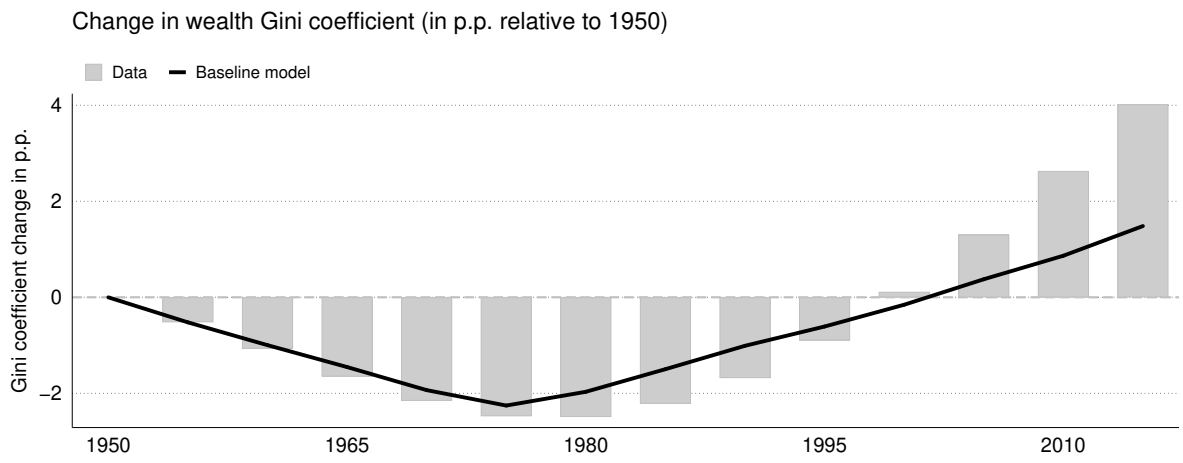

Note: We use household wealth data, measured as net assets, from the extended sample of the Survey of Consumer Finances (SCF, Kuhn et al., 2020). Observations with negative assets are excluded, as the model imposes a non-negativity constraint on asset accumulation. Population weights are applied to the SCF data, and observations are grouped into five-year bins. In the model, probability mass is similarly applied as weights. The black line represents the change in the wealth Gini coefficient in the model (measured in percentage points relative to 1950), while the gray bars show the change in the wealth Gini coefficient derived from the SCF data.

From 1950 to 1975, the wealth Gini coefficient in the data declines by approximately three points, a trend that the model successfully reproduces. Between 1975 and 2015, the wealth Gini coefficient in the data increases by eight points, with the model explaining more than half of this rise. Overall, the model effectively captures both the reduction in inequality prior to 1975 and its subsequent growth.

Most macroeconomic parameters in the model are directly sourced from observational data. However, the model endogenously determines the interest rate, hours worked, the size of social security. We can also compare the ratio of bequests to GDP. For the interest rate, our baseline simulation captures the major trends and some fluctuations observed over time. The data show a decline in interest rates from approximately 8% in 1950 to just over 7% in 2015. In our model, this decline is slightly more pronounced, with the rate falling to just below 7%, see Figure D.1 in Online Appendix D.[10]

Our baseline simulation matches the long-run behavior of average hours worked per capita observed in the data. In particular, consistent with the evidence for the U.S in Boppart and Krusell (2020), average hours in the model do not exhibit any long-run trend. The model generates slightly larger fluctuations in hours than in the data and cannot reproduce behavior of hours inflicted by the Great Recession, see Figure D.2 in Online Appendix D.

The model replicates both the levels and the time variation of the GDP share of pension benefit expenditures very well. Additionally, the future path of benefits implied by our model aligns closely with projections from the Congressional Budget Office. In Figure D.3 of Online Appendix D, we plot the time evolution of the model's pension benefit expenditures against data from the U.S. Social Security Administration. Finally, the average ratio of bequests to GDP in the model is slightly above 5%; further details are provided in Online Appendix D.

Futher, we examine the Gini coefficient and Lorenz curves for income generated by the model

[10]Our model does not include government debt to avoid the arbitrary *ad hoc* assumptions about its evolution in counterfactual scenarios. Consequently, the increased savings in our model result in a more pronounced "savings glut" mechanism compared to the data.

and compare them with observational data from the PSID, aggregated by decades for the 1970s, 1980s, 1990s, 2000s, and 2010s. The model closely replicates the observed income distribution, despite income inequality not being a direct target during calibration. While income shocks and life cycle patterns were estimated from PSID data, additional features of the income process, such as the college premium and college shares, were derived from external sources,[11] see Figure D.4 in the Online Appendix D.

Finally, we compare the composition of changes in wealth inequality as represented by the model with the data. Using the extended SCF sample provided by Kuhn et al. (2020), we decompose a Generalized Entropy measure of inequality into between-cohort and within-cohort components. Although the data show larger magnitudes than the model, the patterns produced by the model align remarkably well with empirical regularities, see Figure D.5 in the Online Appendix D.

5 Results

In this section, we show the results of our study. We start by describing the contribution of rising longevity to wealth inequality since 1950 and compare it with other important factors discussed in the literature, such as taxes and incomes.

5.1 Rising longevity and evolution of wealth inequality

We begin by examining the impact of rising longevity on wealth inequality. One significant driver is the composition (structural) effect, which arises because the distribution of assets across age groups typically follows a hump-shaped pattern. In any life-cycle economy, even if agents are identical in all aspects except age, the Gini coefficient will exceed zero. As population ages, the share of younger individuals with fewer assets declines, while the proportion of older individuals nearing retirement, who hold more assets, increases. This shift affects the Gini coefficient, though the magnitude and direction of its impact depend on quantitative factors.

Another critical factor is the behavioral effect, which stems from increasing life expectancy. As individuals plan for longer retirement periods, they adjust their savings behavior, accumulating more assets over their lifetimes. This increased saving intensifies the disparity between younger individuals and those nearing retirement, thereby contributing to rising wealth inequality. Evidence supporting this effect is provided by Bauluz and Meyer (2024).

To quantify these effects, we simulate a counterfactual scenario in which mortality rates are fixed at their 1955 levels and compare it to the baseline scenario, where mortality rates evolve as observed historically. The initial conditions are identical, given by the same initial steady state at $t = 0$ (corresponding to the year 1935). The respective paths of mortality rates in the baseline and counterfactual scenarios are revealed at $t = 1$ (year 1940). The resulting population structures for both scenarios are presented in Figure C.1 in Online Appendix C. Figure 2 shows the evolution of the wealth Gini coefficient under these two scenarios.

[11] Note that we estimate a process for idiosyncratic productivity shocks, not for the entire labor income. Given this process and aggregate variables, labor supply is chosen optimally by the agents within the model. The ability of the model to replicate the observed income distribution means that the model can generate comovement between hourly wages and hours worked consistent with the data.

Figure 2: Baseline vs counterfactual scenario of constant longevity

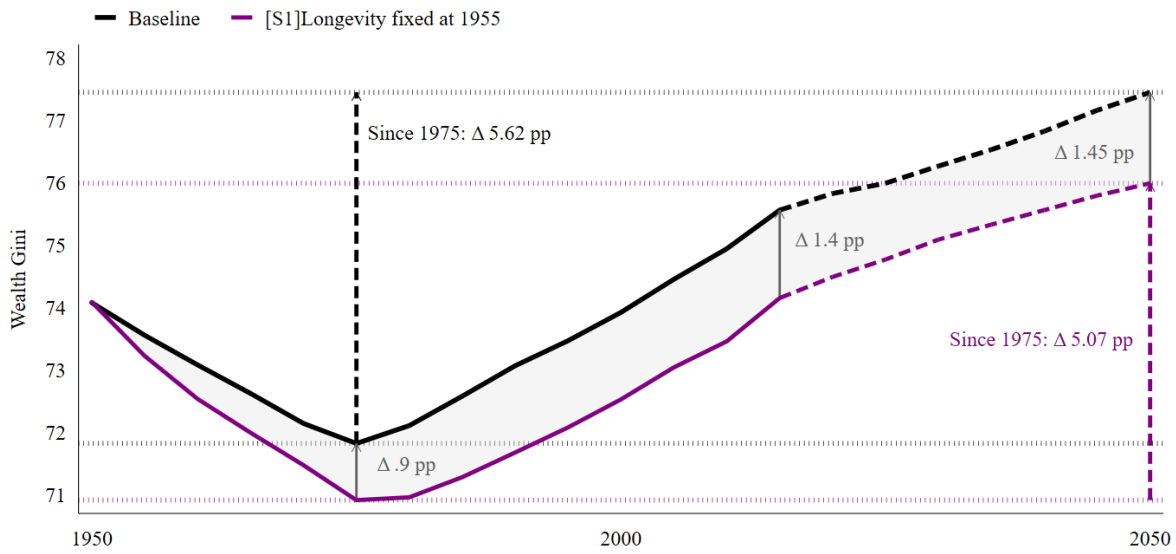

Note: The black line shows the level of the wealth Gini coefficient in the baseline model. The violet line illustrates the wealth Gini coefficient from a counterfactual simulation where mortality rates, used both in calculating the population structure and in the consumer problem, are held constant at their 1955 levels, while all other aspects align with the baseline simulation.

In the absence of changes in longevity, the Gini coefficient declines by 0.9 points more between 1950 and 1975 than in the baseline scenario, as illustrated by the difference between the two lines in Figure 2. This suggests that rising longevity during this period increased wealth inequality by nearly one point. After 1975, rising longevity continues to drive inequality upward, with their cumulative impact reaching approximately 1.5 points by 2015 and 2050.

To disentangle the relative contributions of demographic factors to wealth inequality, we construct a bar graph in Figure 3 (scenario [S1]Longevity:1955). This analysis is based on a comparison between the baseline scenario and a counterfactual scenario with fixed mortality rates, both depicted in Figure 2. In this context, $\boldsymbol{G}_t^b$ represents the wealth Gini coefficient from the baseline model, while $\boldsymbol{G}_t^c$ denotes the coefficient from the counterfactual scenario. The differences between the two scenarios for a given period t are calculated as $\Delta_t = \boldsymbol{G}_t^b - \boldsymbol{G}_t^c$, and these differences are visualized as bars in Figure 3 for $t \in \{1975, 2015, and 2050\}$ are 0.9, 1.4, and 1.45 Gini points, respectively (corresponding to the differences between the two lines in Figure 2). A positive bar value indicate that a factor increases wealth inequality, while a negative values reflects mitigating effect.

Figure 3: Impact of rising longevity on wealth inequality (in Gini points)

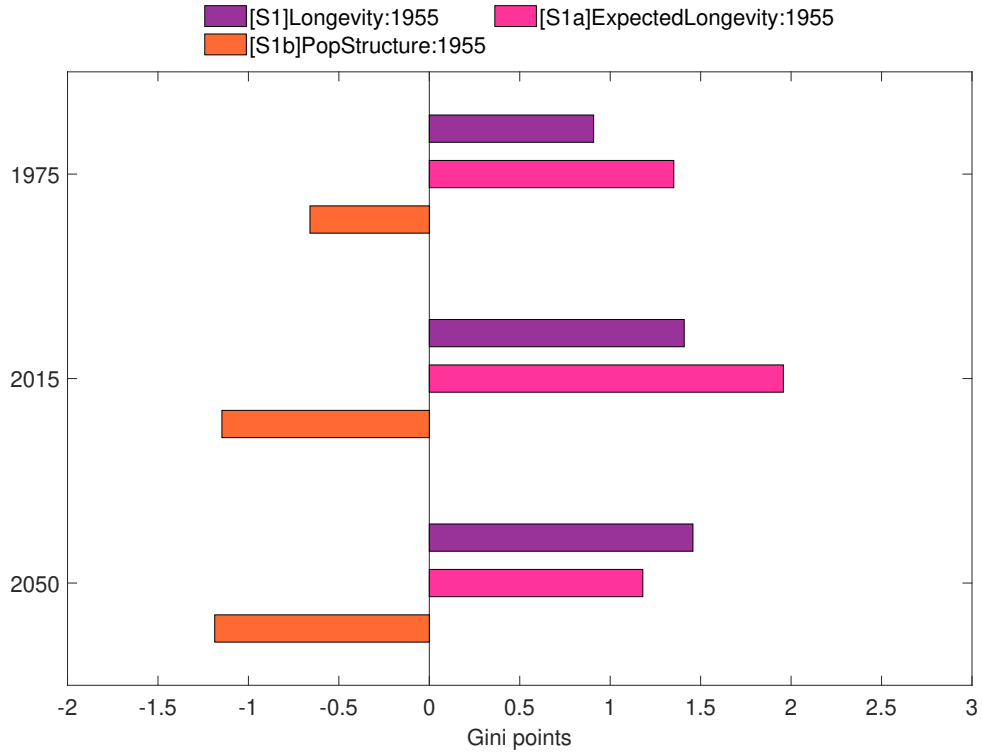

Note: The bars depict the differences in the wealth Gini coefficient for a given year between the baseline scenario and the respective counterfactual scenarios, as defined by the formula $\Delta_t = \boldsymbol{G}_t^b - \boldsymbol{G}_t^c$. A positive value indicates that a given factor contributed to the increase of the Gini coefficient, while a negative value indicates a decrease. The counterfactual scenarios are defined as follows. [S1]Longevity:1955 This scenario fixes mortality rates at their 1955 levels for both population structure and the consumer problem, while all other aspects remain as in the full model. [S1a]ExpectedLongevity:1955 This scenario fixes only the mortality rates in the consumer problem at their 1955 levels, with all other aspects unchanged from the full model. [S1b]PopStructure:1955 This scenario fixes the mortality rates used to compute the population structure at their 1955 levels, while the rest of the model remains unchanged.

To further isolate the composition and behavioral effects, we perform two counterfactual simulations. The [S1a]ExpectedLongevity:1955 scenario fixes mortality rates in the consumer problem, isolating the behavioral effect. The [S1b]PopStructure:1955 scenario fixes mortality rates in population structure, isolating the composition effect. Our analysis reveals that these two effects influence inequality in opposite ways. The behavioral effect amplifies wealth inequality, with greater asset accumulation to fund longer retirements, the gap between younger individuals and those nearing retirement widens. In contrast, the composition effect reduces wealth inequality, with changing age distribution of the population there is fewer younger individuals (who hold limited assets) and more older individuals (who hold substantial assets). However, the behavioral effect outweighs the composition effect, leading to a net rise in wealth inequality.

5.2 Relative importance of rising longevity for wealth inequality

We compare the size of the effects driven by demographics with other key factors identified in the literature. Figure 4 shows the contributions of changes in income inequality, taxes, and technology to wealth inequality. For reference, the figure also includes the contribution of the demographic transition.

To quantify these effects, we simulate a counterfactual scenario in which the relevant parameters are fixed at their 1955 levels and compare it to the baseline scenario, where those parameters evolve

as observed historically. In both scenarios, the initial conditions are identical, based on the same initial steady state at $t = 0$ (corresponding to the year 1935). The respective paths of mortality rates in the baseline and counterfactual scenarios are revealed at $t = 1$ (year 1940).

To start, we analyze the impact of observed trends in income inequality, which reveal three notable developments between 1950 and 2015. First, the share of college graduates increased, which can influence income and wealth inequalities in varying ways. It may reduce inequality by narrowing educational gaps and expanding opportunities, but if the returns to higher education are substantial, it could instead exacerbate inequality.

Second, the college premium rose, amplifying income and wealth inequalities by widening the earnings gap between college graduates and non-graduates. However, it may also have bolstered the wealth of the middle class, potentially offsetting its inequality-enhancing effects.

Figure 4: Impact of different factors evolution on wealth inequality (in Gini points)

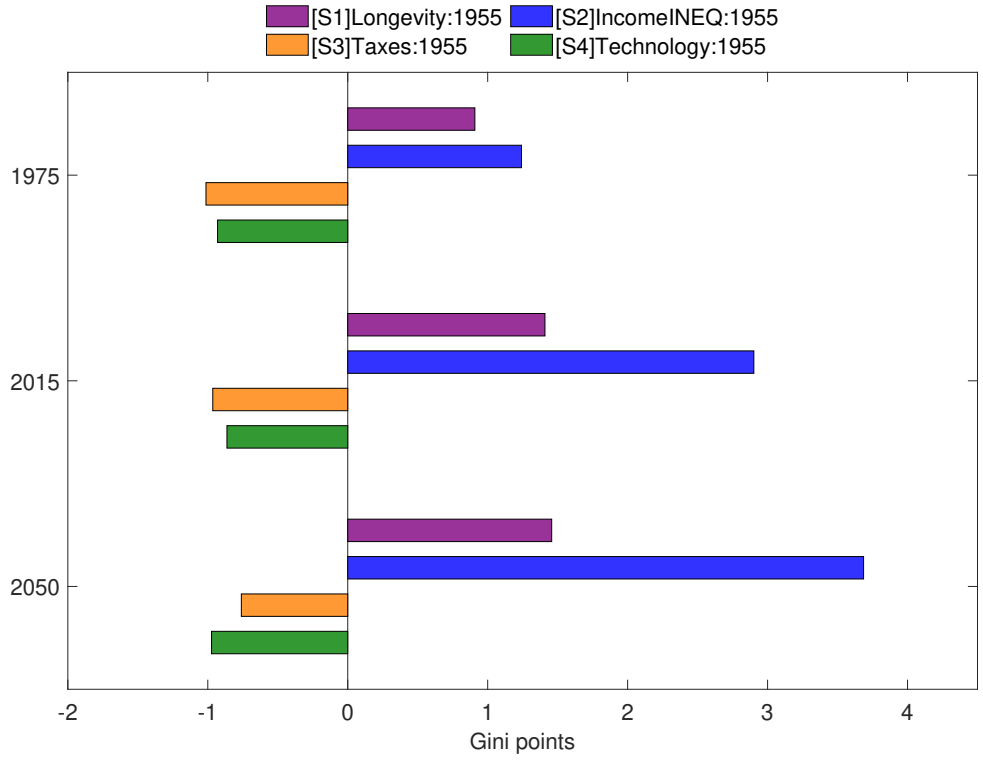

Note: The bars depict the differences in the wealth Gini coefficient for a given year between the baseline scenario and the respective counterfactual scenarios, as defined by the formula $\Delta_t = \boldsymbol{G}_t^b - \boldsymbol{G}_t^c$. The positive/negative number signifies that a given factor contributed to the increase/decrease of the Gini coefficient. Counterfactual scenario [S1]Longevity:1955 was computed by fixing the mortality rates used to compute both the population structure and in the consumer problem at the level from 1955, the rest is as in the full model. Counterfactual scenario [S2]IncomeINEQ:1955 was computed by fixing income characteristics at the 1955 levels, see Figures B.1, B.3 and B.5, the rest is as in the full model. Counterfactual scenario [S3]Taxes:1955 was computed by fixing tax rates at the 1955 levels, see Figure B.7. Counterfactual scenario [S4]Technology:1955 was computed by fixing the TFP growth rate, depreciation rate, and labor share at the 1955 levels, see Figure B.6.

Third, income risk increased for both college graduates and individuals without a college education. This had opposing effects: greater income dispersion contributed to rising wealth inequality, while heightened income risk encouraged precautionary savings, particularly among those with fewer assets, which mitigated wealth inequality. Details on the baseline and counterfactual inputs for these analysis are provided in Online Appendix B. The overall impact of these three factors on the Gini wealth coefficient ultimately depends on the quantitative analysis.

In Figure 4, the counterfactual scenario [S2]IncomeINEQ:1955 demonstrates the impact of these income changes. This scenario fixes income characteristics at their 1955 levels.[12] Our simulations reveal that income changes are the primary driver of wealth inequality over time. However, rising longevity has a substantial impact, with their effect being approximately half that of income changes. By 1975, income changes increase the Gini coefficient by approximately 1.2 points, while rising longevity accounts for a smaller increase of about 0.9 points. By 2015, income changes contribute 2.9 Gini points, compared to 1.4 points from rising longevity. By 2050, income changes raise the Gini coefficient by 3.7 points, while demographic factors account for 1.45 points.

These results highlight the critical role of income inequality and rising longevity in shaping wealth inequality over time. Although income changes exhibit a larger and increasing effect, the impact of rising longevity remains considerable. We present detailed analysis concerning the contributions of specific income components to inequality in Online Appendix E.1.

Our results align with findings in the literature that identify income inequality as a primary driver of wealth inequality, as demonstrated by studies such as Castaneda et al. (2003) and Kindermann and Krueger (2022). The contribution of our study is its explicit consideration and quantification of the role for rising longevity in shaping wealth inequality inequality trends. We provide a more comprehensive view of the underlying drivers of this phenomenon, by showing that changes in life expectancy and population structure play an important role in explaining wealth inequality over time.

Another key determinant of wealth inequality is taxation.[13] Figure 4 presents the counterfactual scenario [S3]Taxes:1955, which examines the impact of tax changes by holding tax rates constant at their 1955 levels (see Figure B.7), while all other elements of the model remain unchanged. Our simulations show that changes in taxation reduce the Gini coefficient by 1 point in 1975. Although the effect persists beyond this period, it diminishes slightly, contributing to reductions of just under 1 point in 2015 and 0.8 points in 2050.

The impact of demographic factors contrasts with that of taxation, as rising longevity increases inequality, while taxation reduces it. The quantitative effect of demographic factors is also slightly larger than that of taxation. Our findings regarding tax changes are also consistent with the existing literature. For example, Hubmer et al. (2021), who do not account for demographic effects, identify the decline in tax progressiveness during the late 1970s as a primary driver of rising wealth inequality. Although our model does not single out tax changes as the key driver of wealth inequality, the qualitative effects of income tax progressiveness align with their conclusions. As shown in the Online Appendix E.2, increased labor tax progressiveness contributed to a decline in wealth inequality by 1975. However, the subsequent decline in progressiveness resulted in rising wealth inequality. This ongoing trend of declining tax progressiveness has historically intensified wealth inequality and is expected to continue doing so in the future.

Finally, we examine the impact of technological changes. The counterfactual scenario denoted as [S4]Technology:1955 captures these effects by fixing the TFP growth rate, depreciation rate, and labor income share at their 1955 levels (for more details, refer to Figure B.6). Our simulations show that technological changes reduce wealth inequality, lowering the wealth Gini coefficient by 0.9 points in both 1975 and 2015, and by 1.0 point in 2050. We present a detailed analysis in Online Appendix E.3.

Although the contribution of rising longevity is smaller than that of income dynamics across all periods, it remains considerable. In contrast, the effect of tax changes is somewhat less pronounced.

[12] Income risk (the variance of idiosyncratic productivity shocks) is held at its initial level, based on estimates for cohorts entering the labor market between 1950 and 1954.

[13] Here we present the effects of changes in all taxes. Online Appendix E.2 offers details on how different taxes affect wealth inequality.

While much of the literature has focused on the roles of income evolution and tax policy in shaping wealth inequality, the impact of rising longevity has received less attention. Our results show the important role of demographic factors.

Sensitivity analyses To assess the robustness of our results, we conduct a series of sensitivity checks, detailed in Online Appendix F. These checks specifically examine whether the contribution of demographic factors to wealth inequality changes under alternative assumptions.

First, we test the sensitivity of our results to calibration of the inverse elasticity of intertemporal substitution, θ, which also determines risk aversion (Online Appendix F.1). Second, we introduce persistent differences in interest rates between college-educated individuals and those with less than a college education (Online Appendix F.2). Third, we remove discount factor shocks to assess their influence (Online Appendix F.3). Fourth, we use an alternative formulation of the income process (Online Appendix F.4). Fifth, we assume a higher projected TFP growth rate for the future (Online Appendix F.5). Finally, we allow for unequal distribution of bequests (Online Appendix F.6). Rising longevity consistently contributes to increasing wealth inequality in these experiments, increasing the wealth Gini coefficient by approximately 1 point in 1975 and by nearly 1.5 points in both 2015 and 2050.

Despite robustness, our results are not without limitations. First, while our model replicates an important part of wealth inequality dynamics, the rise in wealth inequality in the recent decade is larger than implied by our model and macroeconomic inputs. This may be related to increasing financialization, the permeation of demographic factors additionally to rising longevity, etc. Second, due to the general equilibrium structure, our model ignores the endogeneity of dimensions such as education and returns to skills. Finally, models with dynasties can help to explain persistently high and low wealth.

6 Conclusions

The sources of wealth inequality, particularly the post-1970s rise in the U.S., remain a subject of considerable debate. Much of the applied macroeconomic literature attributes this increase to growing income inequality and a decline in redistribution within the tax system. This study focuses explicitly on the role of rising old age longevity, analyzed through the lens of an overlapping generations general equilibrium model. Although we incorporate the channels identified in previous research, we also quantify the impact of rising longevity. Our findings indicate that increased longevity contributed to nearly a 1 Gini point increase in wealth inequality in the U.S. by 1975 and nearly 1.5 Gini points by 2015. Additionally, using demographic projections, we demonstrate that these mechanisms are expected to further drive wealth inequality upward in the coming decades.

This substantial role of demographics is primarily attributed to the behavioral channel. As individuals expect to live longer in old age, they adjust their asset accumulation and decumulation patterns, significantly affecting both the general equilibrium of this economy and the distribution of wealth and income. This behavioral effect is stronger than the impact of changes in population structure.

Our model incorporates carefully calibrated mechanisms discussed in the existing literature, enabling counterfactual simulations to evaluate the relative importance of income inequality, tax channels, and demographics. In the OLG framework, we find that the tax channel plays a relatively minor role, and its ability to offset the rise in wealth inequality will remain fairly limited. Additionally, we show that the evolving nature of work, coupled with rising income inequality, will further amplify wealth inequality in the future, compounding the effects of rising longevity.

References

Aguiar, M., Bils, M., and Boar, C. (2024). Who are the hand-to-mouth? *The Review of Economic Studies*.

Aiyagari, S. R. (1994). Uninsured Idiosyncratic Risk and Aggregate Saving. *The Quarterly Journal of Economics*, 109(3):659–684.

Aoki, S. and Nirei, M. (2017). Zipf's Law, Pareto's Law, and the Evolution of Top Incomes in the United States. *American Economic Journal: Macroeconomics*, 9(3):36–71.

Auclert, A., Malmberg, H., Martenet, F., and Rognlie, M. (2021). Demographics, wealth, and global imbalances in the twenty-first century. NBER Working Paper 29161.

Autor, D., Goldin, C., and Katz, L. F. (2020). Extending the race between education and technology. *AEA Papers and Proceedings*, 110:347–51.

Bach, L., Calvet, L. E., and Sodini, P. (2020). Rich pickings? risk, return, and skill in household wealth. *American Economic Review*, 110(9):2703–47.

Barro, R. J. and Sahasakul, C. (1983). Measuring the Average Marginal Tax Rate from the Individual Income Tax. *The Journal of Business*, 56(4):419–452.

Bauluz, L. and Meyer, T. (2024). The wealth of generations. WID Working Paper 2024/04, WID - World Inequality Lab.

Benhabib, J., Bisin, A., and Luo, M. (2019). Wealth Distribution and Social Mobility in the US: A Quantitative Approach. *American Economic Review*, 109(5):1623–1647.

Benhabib, J., Bisin, A., and Zhu, S. (2011). The distribution of wealth and fiscal policy in economies with finitely lived agents. *Econometrica*, 79(1):123–157.

Bewley, T. (1977). The permanent income hypothesis: A theoretical formulation. *Journal of Economic Theory*, 16(2):252–292.

Bielecki, M., Brzoza-Brzezina, M., and Kolasa, M. (2020). Demographics and the natural interest rate in the euro area. *European Economic Review*, 129(C).

Boppart, T. and Krusell, P. (2020). Labor supply in the past, present, and future: A balanced-growth perspective. *Journal of Political Economy*, 128(1):118–157.

Cagetti, M. and De Nardi, M. (2006). Entrepreneurship, frictions, and wealth. *Journal of Political Economy*, 114(5):835–870.

Case, A. and Deaton, A. (2021). Life expectancy in adulthood is falling for those without a ba degree, but as educational gaps have widened, racial gaps have narrowed. *Proceedings of the National Academy of Sciences*, 118(11):e2024777118.

Castaneda, A., Diaz-Gimenez, J., and Rios-Rull, J.-V. (2003). Accounting for the U.S. Earnings and Wealth Inequality. *Journal of Political Economy*, 111(4):818–857.

Chetty, R., Grusky, D., Hell, M., Hendren, N., Manduca, R., and Narang, J. (2017). The fading American dream: Trends in absolute income mobility since 1940. *Science*, 356(6336):398–406.

De Nardi, M. (2004). Wealth Inequality and Intergenerational Links. *Review of Economic Studies*, 71(3):743–768.

Deaton, A. and Paxson, C. (2000). Growth and saving among individuals and households. *Review of Economics and Statistics*, 82(2):212–225.

Eggertsson, G. B., Mehrotra, N. R., and Robbins, J. A. (2019). A Model of Secular Stagnation: Theory and Quantitative Evaluation. *American Economic Journal: Macroeconomics*, 11(1):1–48.

Epper, T., Fehr, E., Fehr-Duda, H., Kreiner, C. T., Lassen, D. D., Leth-Petersen, S., and Rasmussen, G. N. (2020). Time discounting and wealth inequality. *American Economic Review*, 110(4):1177–1205.

Fagereng, A., Guiso, L., Malacrino, D., and Pistaferri, L. (2020). Heterogeneity and persistence in returns to wealth. *Econometrica*, 88(1):115–170.

Fagereng, A., Holm, M. B., Moll, B., and Natvik, G. (2019). Saving behavior across the wealth distribution: The importance of capital gains. NBER Working Paper 26588.

Gabaix, X., Lasry, J.-M., Lions, P.-L., and Moll, B. (2016). The dynamics of inequality. *Econometrica*, 84(6):2071–2111.

Gagnon, E., Johannsen, B. K., and López-Salido, D. (2021). Understanding the new normal: The role of demographics. *IMF Economic Review*, 69(2):357–390.

Gomez, M. (2023). Decomposing the Growth of Top Wealth Shares. *Econometrica*, 91(3):979–1024.

Gomez, M. (2024). Wealth inequality and asset prices. *mimeo*.

Gomez, M. and Gouin-Bonenfant, E. (2024). Wealth inequality in a low rate environment. *Econometrica*, 92(1):201–246.

Guvenen, F., Kaplan, G., Song, J., and Weidner, J. (2022). Lifetime incomes in the united states over six decades. 14(4):446–479.

Hubmer, J., Krusell, P., and Smith., A. A. (2021). Sources of us wealth inequality: Past, present, and future. *NBER Macroeconomics Annual*, 35:391–455.

Kaymak, B. and Poschke, M. (2016). The evolution of wealth inequality over half a century: The role of taxes, transfers and technology. *Journal of Monetary Economics*, 77(C):1–25.

Kindermann, F. and Krueger, D. (2022). High marginal tax rates on the top 1 percent? lessons from a life-cycle model with idiosyncratic income risk. *American Economic Journal: Macroeconomics*, 14(2):319–366.

Krueger, D. and Ludwig, A. (2007). On the consequences of demographic change for rates of returns to capital, and the distribution of wealth and welfare. *Journal of Monetary Economics*, 54(1):49–87.

Kuhn, M., Schularick, M., and Steins, U. I. (2020). Income and wealth inequality in America, 1949–2016. *Journal of Political Economy*, 128(9):3469–3519.

Lippi, F. and Perri, F. (2023). Unequal growth. *Journal of Monetary Economics*, 133:1–18.

Lusardi, A., Michaud, P.-C., and Mitchell, O. S. (2017). Optimal financial knowledge and wealth inequality. *Journal of Political Economy*, 125(2):431–477.

McDaniel, C. (2007). Average tax rates on consumption, investment, labor and capital in the oecd: 1950-2003. *mimeo*.

McGrattan, E. and Prescott, E. (2017). On financing retirement with an aging population. *Quantitative Economics*, 8(1):75–115.

Mendoza, E. G., Razin, A., and Tesar, L. L. (1994). Effective tax rates in macroeconomics: Cross-country estimates of tax rates on factor incomes and consumption. *Journal of Monetary Economics*, 34(3):297–323.

Mertens, K. and Montiel Olea, J. L. (2018). Marginal tax rates and income: New time series evidence. *The Quarterly Journal of Economics*, 133(4):1803–1884.

Piketty, T., Saez, E., and Zucman, G. (2018). Distributional national accounts: methods and estimates for the United States. *The Quarterly Journal of Economics*, 133(2):553–609.

Saez, E. and Zucman, G. (2016). Wealth inequality in the United States since 1913: Evidence from capitalized income tax data. *Quarterly Journal of Economics*, 131(2):519–578.

Straub, L. (2019). Consumption, savings, and the distribution of permanent income.

Zeldes, S. P. (1989). Consumption and liquidity constraints: An empirical investigation. *Journal of Political Economy*, 97(2):305–346.

Online Appendix:

Demographic transition and the rise of wealth inequality

By Krzysztof Makarski, Joanna Tyrowicz and Piotr Żoch

Contents

A Online Appendix: the model

In this section we present details of our general equilibrium OLG model with heterogeneous households that were relegated from the main text to the Online Appendix.

A.1 Social security

Post-retirement ($j > \bar{j}$), benefits grow at the same rate as the aggregate labor income in the economy. Thus benefits are given by:

$$b_{s,\bar{j},t} = \varrho_{\bar{j},t} \cdot p_{\bar{j},t} \cdot f_{s,\bar{j},t} \overline{w_t e_t \ell_t} \quad \text{and} \quad b_{s,j,t} = \frac{w_t L_t}{w_{t-1} L_{t-1}} b_{s,j-1,t-1} \text{ for } j > \bar{j}. \tag{A.1}$$

Drawing rights (average lifetime earnings relative to average earnings in the economy) $f_{s,j,t}$ evolve according to

$$f_{s,j+1,t+1} = \frac{1}{j} \left((j-1) \cdot f_{s,j,t} + \frac{\min \left\{ w_t e_{s,j,t} \ell_{s,j,t}, \mathsf{cap}_t \right\}}{\overline{w_t e_t \ell_t}} \right), \tag{A.2}$$

where cap_t denotes the OASDI cap, expressing earnings relative to average economy earnings over a lifetime. We compute AIME for the whole working period rather than the 35 highest-earnings, consistent with 5-year periods and prior literature (Nishiyama and Smetters, 2007; McGrattan and Prescott, 2017).

The replacement rate $p_{\bar{j},t}$ is computed according to

$$p_{\bar{j},t} = 0.9 \cdot \min \left\{ 1, \frac{F_{1,t}}{f_{s,\bar{j},t}} \right\} + 0.32 \cdot \min \left\{ 1 - \frac{F_{1,t}}{f_{s,\bar{j},t}}, \frac{F_{2,t}}{f_{s,\bar{j},t}} \right\} + 0.15 \max \cdot \left(1 - \frac{F_{2,t}}{f_{s,\bar{j},t}}, 0 \right)$$

where bend points $(F_{1,t}, F_{2,t})$ reflect the progressive replacement rates and are expressed as a fraction of average earnings (McGrattan and Prescott, 2017).

A.2 Production

Our model features a standard Cobb-Douglas production function $Y_t = K_t^{\alpha_t} \left(A_t L_t \right)^{1-\alpha_t}$ with labor augmenting technological progress where $A_{t+1}/A_t = 1 + \gamma_{t+1}^A$. The standard profit maximization problem of the firm yields the following factor prices

$$r_t = \alpha_t K_t^{\alpha_t - 1} \left(A_t L_t \right)^{1-\alpha_t} - d_t \quad \text{and} \quad w_t = \left(1 - \alpha_t \right) K_t^{\alpha_t} A_t^{1-\alpha_t} L_t^{-\alpha_t}, \tag{A.3}$$

Gross capital return $r_t + d_t$ is taxed at the rate $\tau_{k,t}$ so that the after-tax rate of return on capital is

$$\tilde{r}_t = \left(1 - \tau_{k,t} \right) \left(r_t + d_t \right) - d_t. \tag{A.4}$$

A.3 Government

The tax revenue T_t is used to finance spending on government purchases G_t and to subsidize the social security system, $\mathcal{S}_t$:

$$G_t + \mathcal{S}_t = T_t, \tag{A.5}$$

where

$$T_t = \sum_{s \in \{L,H\}} \sum_{j=1}^{\bar{j}-1} N_{s,j,t} \int_\Omega \mathcal{T}_t \left(y_{s,j,t} \left(z_{s,j,t} \right), \bar{y}_t \right) d\mathbb{P}_{s,j,t} + \tau_{k,t} \left(r_t + d_t \right) K_t + \tau_{c,t} C_t. \tag{A.6}$$

Here C_t denotes aggregate consumption, $C_t = \sum_{s\in\{L,H\}} \sum_{j=1}^{J} N_{s,j,t} \int_\Omega c_{s,j,t}\left(z_{s,j,t}\right) d\mathbb{P}_{s,j,t}$, and $\mathbb{P}_{s,j,t}$ is the probability measure describing the distribution of agents of education level s and age j in period t over the state space Ω.

The subsidy to the social security system $\mathcal{S}_t$ is equal to the difference between the total pension benefit payments and the total contributions:

$$\mathcal{S}_t = \sum_{s\in\{L,H\}} \sum_{j=\bar{j}}^{J} N_{s,j,t} \int_\Omega b_{j,t}\left(z_{s,j,t}\right) d\mathbb{P}_{s,j,t} - \tau_{ss,t} w_t L_t. \tag{A.7}$$

We assume that the model is closed by government expenditure G_t.

A.4 Equilibrium

Given government policies $\left\{\tau_{c,t}, \tau_{k,t}, \tau_{\ell,t}\lambda_t, \tau_{ss,t}, \mathcal{S}_t, \varrho_{\bar{j},t}\right\}_{t=0}^{\infty}$ a competitive equilibrium is a sequence of: i) value functions $\left\{\left(V_{s,j,t}\left(z_{s,j,t}\right)\right)_{j=1}^{J}\right\}_{t=0}^{\infty}$ for $s \in \{L,H\}$; ii) policy functions $\left\{\left(c_{s,j,t}\left(z_{s,j,t}\right), \ell_{s,j,t}\left(z_{s,j,t}\right), f_{s,j+1,t+1}\right.\right.$ for $s \in \{L,H\}$; iii) prices $\{r_t, w_t\}_{t=0}^{\infty}$; iv) aggregate quantities $\{L_t, K_t, Y_t, C_t, G_t, T_t\}_{t=0}^{\infty}$; and v) measures of households $\left\{\left(\mathbb{P}_{s,j,t}\right)_{j=1}^{\infty}\right\}_{t=0}^{\infty}$ for $s \in \{L,H\}$ such that:

- **firm problem:** for each t, prices $\{r_t, w_t\}$ satisfy equations (A.3);
- **household problem:** for each s, j, t value functions $V_{s,j,t}\left(z_{s,j,t}\right)$ and policy functions $c_{s,j,t}\left(z_{s,j,t}\right), \ell_{s,j,t}\left(z_{s,j,t}\right), .$ solve the problem (2);
- **government:** the government budget and the pension system constraints are satisfied, i.e., equations (A.5) and (A.7) are satisfied;
- **markets clear:**

$$\begin{aligned}
\text{labor market:} \qquad & L_t = \sum_{s\in\{L,H\}} \sum_{j=1}^{\bar{j}-1} N_{s,j,t} \int_\Omega e_{s,j,t}\left(z_{s,j,t}\right) \ell_{s,j,t}\left(z_{s,j,t}\right) d\mathbb{P}_{s,j,t} \\
\text{asset market:} \qquad & K_{t+1} = \sum_{s\in\{L,H\}} \sum_{j=1}^{J} N_{s,j,t} \int_\Omega a_{s,j+1,t+1}\left(z_{s,j,t}\right) d\mathbb{P}_{s,j,t} \\
\text{goods market:} \qquad & Y_t = C_t + K_{t+1} - \left(1 - d_t\right) K_t + G_t
\end{aligned}$$

- **probability measures:** measures of households $\left\{\left(\mathbb{P}_{s,j,t}\right)_{j=1}^{\infty}\right\}_{t=0}^{\infty}$ for $s \in \{L,H\}$ are consistent with exogenous processes for productivity, discount factors and returns, and policy functions.

B Online Appendix: calibration

In this section we present the details of our baseline calibration, with data sources and intermediary steps. We also describe how we arrive at counterfactual calibration of the model parameters.

B.1 Demographics

We use population data from Centers for Disease Control and Prevention (CDC). The five-year averages for births and survival probabilities are provided by the United Nations Population database. This data covers historical births and survival probabilities as well as provides a demographic forecast until 2100. We assume that after that year the birth rate continues at the same level, equal to 0.06% per year. We also assume that survival probabilities stabilize at their 2100 levels.

The share of households with $s = H$ in each birth cohort is set to match the share of individuals with at least four years of college completed by the age of twenty-five in the U.S. Census and American Community Survey. This data covers cohorts born in the years 1915-1995. We obtain the trend component by applying the Hodrick-Prescott filter of the series and then calculate five-year averages of the trend component. When we extrapolate into the future, we aim for the smoothness of calibration. We assume that the trend share increases from 35% in 2020 to 40% in 2030 and then gradually grows to reach 44.5% by 2100.[14] The path of the share of households with a college education in each birth cohort that we use as an input for the model is shown in Figure B.1. The extrapolated share of college graduates is smooth and continues the observed trend.

Figure B.1: Share of college graduates

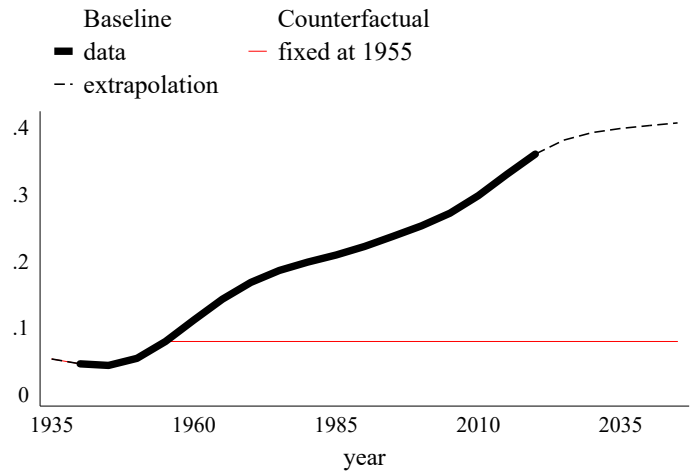

Note: Share of college graduates by the age of 25. from U.S. Census and American Community Survey. The share of college graduates is adjusted to five-year periods by applying Hodrick-Prescott filter with parameter 6.25 and calculating five-year averages of the trend component.

In our model, education status affects mortality risk (in line with empirical evidence, see Chetty et al., 2016). Observational data by Case and Deaton (2021) reveal that mortality for cohorts reaching the age of 50 between 1935 and 1965 was substantially lower for individuals with a college education and that gap was widening especially for the most recent of these birth cohorts, as portrayed in Figure B.2. Note that life expectancy was increasing for all levels of education, but the increase was

[14] We need to assume a constant terminal level in the far future to calculate the final steady state.

more pronounced for individuals with a college education. Individuals from birth cohorts that reach 50 after 1965 are also characterized by a large heterogeneity of mortality rates depending on college education, but here Case and Deaton (2021) rely on demographic projections. They suggest that the gap will eventually narrow.

Figure B.2: Life expectancy at the age of 50 for college, less than college educated

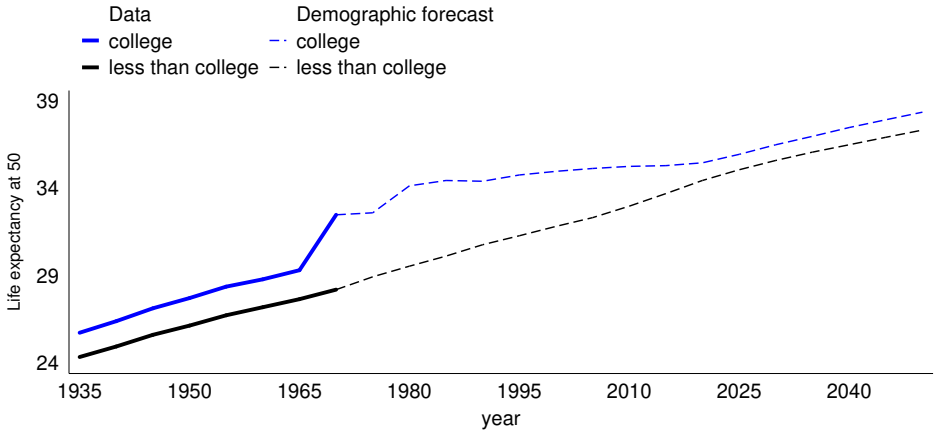

Note: The blue line shows life expectancy at the age of 50 from United Nations Population database. The other two lines show life expectancy at the age 50 for individual with college education and with less than college education. Life expectancy by education status is calculated using data from Case and Deaton (2021). See Section 3.1 for details. Data are adjusted to five-year periods by calculating five-year averages.

The survival probabilities in the model, $\psi_{s,j,t}$, depend on the education level. To capture this heterogeneity, we use U.S. death certificate data from Case and Deaton (2021) which include survival probabilities by cohort, age, and college attainment in years 1990 to 2018. We calculate ratios of survival probabilities of college-educated to survival probabilities of those who do not have a college education. We then use these ratios together with survival probabilities for the entire population and the data on the share of college-educated households to obtain $\psi_{s,j,t}$. For cohorts born before 1915, we extrapolate the ratio of survival probabilities for college-educated individuals relative to those without a college education using the value observed for the 1915 cohort using the first observation in Case and Deaton (2021), that is the ratio is assumed to be 1.018. Analogously, for cohorts born after 1990, we extrapolate the using the value observed for the 1990 cohort, that is 1.006. The extrapolated values of $\psi_{s,j,t}$ additionally depend on the projected survival probabilities for the entire population from the United Nations Population Database and our extrapolation of shares of college graduates. We show life expectancy at the age of 50 for the subsequent birth cohorts in Figure B.2.

B.2 Income

Recall Equation (3) that describes $e_{s,j,t}$: $\ln e_{s,j,t} = \beta_{s,t} + \zeta_{s,j} + \omega_{s,j,t}$. where $\beta_{s,t}$ is a time-varying component common to all households with the same education level s (college premium), $\zeta_{s,j}$ is a type-specific deterministic age profile and $\omega_{s,j,t}$ follows a first-order Markov chain with states $\omega_{s,j,t}$ and transition matrix $\pi^{\omega}_{s,j,t}\left(\omega_{s,j+1,t+1} \mid \omega_{s,j,t}\right)$. In this Appendix we describe how we calibrate each of the three components of $e_{s,j,t}$.

B.2.1 College premium

We normalize $\beta_{L,t} = 1$ and use the (log) college wage premium series from Goldin and Katz (2008), extended in Autor et al. (2020) to 1914-2020 to construct our measure of $\beta_{H,t}$. We calculate the trend component using the Hodrick-Prescott filter. Given that the growth of the trend component slowed down after 2000 and essentially halts around 2015, we assume the college premium will remain constant after 2020. The level of college wage premium we use in our model is shown in Figure B.3.

Figure B.3: Skill premium

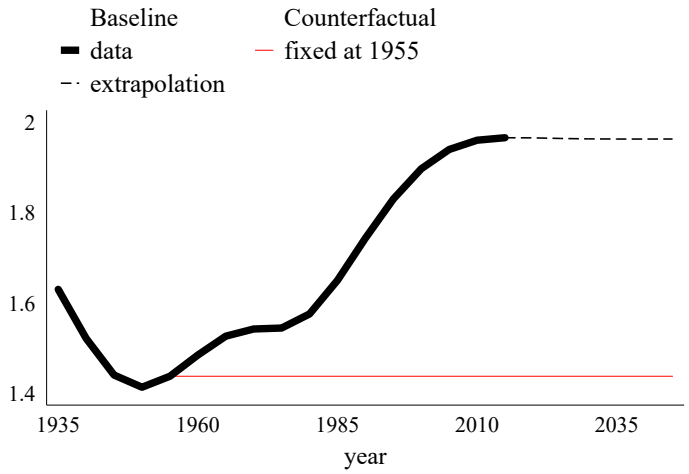

Note: Skill premium from Autor et al. (2020). Skill premium is adjusted to five-year periods by applying Hodrick-Prescott filter with parameter 6.25 and calculating five-year averages of the trend component.

B.2.2 Processing PSID data

We use 1970-2019 waves of the Panel Study of Income Dynamics (PSID) to calibrate type-specific deterministic age profiles $\zeta_{s,j}$ and idiosyncratic income risk $\omega_{s,j,t}$.

Sample selection Our sample consists of households with heads that satisfy the following conditions:

- Older than 19 and younger than 66.
- Provide non-intermittent responses to the survey.
- Appear at least four consecutive times in the panel (after restricting observations, as explained below)

Observations in a particular year are dropped if:

- Household (head + spouse) hourly labor income is greater than \$250 or smaller than \$2 (for variable definitions see below; all nominal variables are deflated to January 2000).
- Annual growth of household hourly labor income is greater than 500% or the annual fall is greater than 80%.
- Household total work hours in a year is lower than 260 hours (5 hours per week).

- Total household labor income is smaller than \$1'000 or greater than \$1'000'000.

Note that a household can be excluded from a sample in a particular year, but still remain in the sample in the other years, as long as it satisfies conditions for at least four consecutive years.

We label households who receive a sufficiently large share of income from businesses in a given period as "superstar". We divide our sample into non-overlapping 5-year periods. We label a household as an "superstar" if in a given 5-year period it satisfies two criteria: 1) its household income over a period has to be above the 25th percentile; 2) the share of 5-year business income in total income has to exceed 25%. Note that if a household is an "superstar" in some periods, we keep observations corresponding to this household in periods in which it is not labeled as an "superstar".

In our baseline specification, we exclude "superstar" when estimating $\zeta_{s,t}$ nor a first-order auto-regressive process (4). We use these observations to compute the share of "superstar" in the economy (as a moment target) and exit rates (as a model parameter).

We study the role of this assumption in Appendix F.4, where we present the alternative calibration of income processes. Specifically, there we do not distinguish entrepreneurs. Instead, we estimate the income process $\zeta_{s,t}$ and a first-order auto-regressive process (4) using all observations jointly. This specification of the model does not have a "superstar" state in the income process.

Variable definitions

- Age – Individuals are assigned to a particular birth cohort by subtracting their age from the year of the last survey in which they appeared. The age in each year is thus calculated based on the cohort (eliminating the possibility that someone had the same age in two consecutive surveys).
- Total household labor income – Sum of spouse and head wages and salaries, bonuses, overtime payments, tips, commissions, professional practice or trade, additional job income, miscellaneous labor income, as well as business income and farm income. Up to 1993 we use two variables which include all above: (i) assets part of business income for both head and spouse (V20439 in 1992), (ii) the rest (in 1993 ER71321 for spouse; V23323 for head). From 1994 we sum the following variables: (i) labor income (in 1994 ER4144 for spouse; ER4140 for head), (ii) S/H part of labor business income (in 1994 V21806 for spouse; ER4119 for head), (iii) S and H part of farm income (ER4117 in 1994), (iv) assets part of business income for head or spouse (in 1993 V21814 for spouse and V21810 for head).
- Total work hours – Sum of spouse and head total annual work hours on all jobs (including overtime).
- Household hourly labor income - Total household labor income divided by total work hours.
- Education – Based on variable indicating highest grade or year of school completed (ER30052 in 1970) education was transformed into categorical variable taking 3 levels: (i) 0-11 grades; (ii) High School or 12 grades and non-academic training; (iii) College dropout, BA degree or higher.

B.2.3 Deterministic age profiles and income risk

Age profile $\zeta_{s,j}$ estimation We recover deterministic age profiles $\zeta_{s,j}$ by applying Deaton and Paxson (2000) decomposition. This method allows for the identification of age effects, controlling for year and cohort effects, such that: 1) the sum of year effects is normalized to 0, and 2) they are

orthogonal to a linear time trend. This assumption overcomes the identification problem (cohort is colinear with age and year) and attributes growth in wages to age and cohort effects, whereas year effects are responsible for cyclical fluctuations. Thus to obtain $\zeta_{s,j}$ we estimate a simple regressions (separately for $s = L$ and $s = H$)

$$\ln w_{i,s,j,t} = \sum_{j=25}^{60} \hat{\zeta}_{s,j} \cdot \text{Age}_{s,j} + \sum_{c=1926}^{1986} \alpha_{s,c} \cdot \text{Cohort}_{s,c} + \sum_{t=1970}^{2019} \gamma_{s,t} \cdot \text{Year}_{s,t} + \epsilon_{i,s,j,t}, \tag{B.1}$$

where $w_{i,s,j,t}$ is hourly household labor income of household i. Households are assigned to a particular birth cohort c by subtracting their age from the year of their last available survey. $\text{Age}_{s,j}$, $\text{Cohort}_{s,c}$ and $\text{Year}_{s,t}$ are dummies which take value one for observations from year t, age j and cohort c. To overcome the issue of colinearity between age, cohort and year we create new year dummies (and use it instead of $\text{Year}_{s,t}$ in regression):

$$d_{s,t} = \text{Year}_{s,t} - \left[(t - 1970) \cdot \text{Year}_{s,1971} - (t - 1971) \cdot \text{Year}_{s,1970}\right].$$

Although we drop $d_{s,1970}$ and $d_{s,1971}$, the values of $\gamma_{s,t}$ for those years can be recovered based on the assumption of their orthogonality to the time trend and the assumption of $\sum_{t=1970}^{2019} \gamma_{s,t} = 0$. We use residuals from regression equation (B.1) in the next step and denote them by ω. Figure B.4a shows the results of estimation. We calculate five-year averages of $\hat{\zeta}_{s,j}$ to use as an input in the model. The results are shown in Figure B.4b.

Figure B.4: Deterministic profile of log productivity across age

(a) Empirical estimates

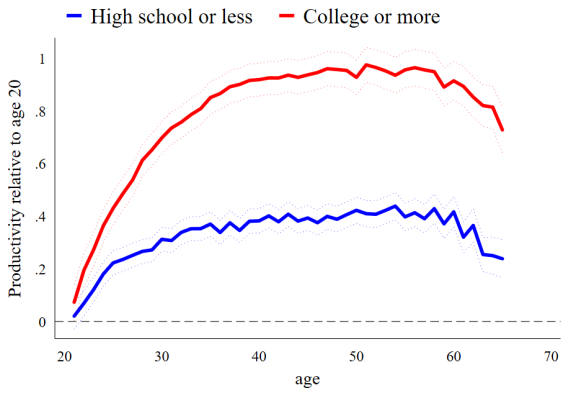

(b) Model inputs

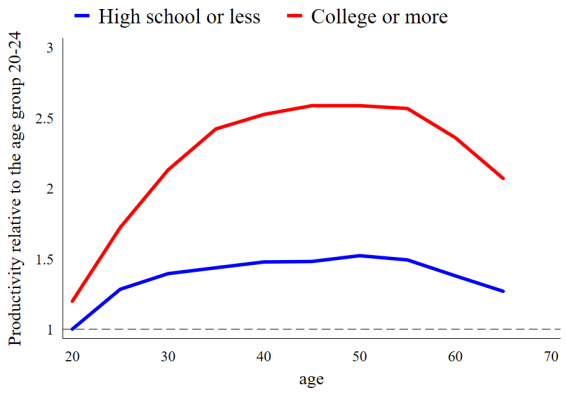

Note: Deterministic profiles of log productivity are calculated using PSID data, with the restrictions described above. The figure shows the estimates $\hat{\zeta}_{s,j}$ from regression equation (B.1), relative to the age of 20 and the level of education "high school or less". As inputs for the model, the deterministic profiles of productivity are calculated by taking $\exp$ of 5-year averages of the point estimates $\hat{\zeta}_{s,j}$. The figure shows $\exp(\zeta_{s,j})$, relative to the age of 20-24 and the level of education "high school or less".

Income process estimation We use the residuals from regression (B.1) as our measure of idiosyncratic productivity. Use $\omega_{i,s,c,t}$ to denote the level of idiosyncratic productivity in year t for individual i of type s, born in year c. We assume

$$\omega_{i,s,c,t} = \varrho_{\omega,s}\omega_{i,s,c,t-1} + \varepsilon_{\omega,i,s,c,t}, \quad \varepsilon_{\omega,i,s,c,t} \sim N\left(0, \sigma^2_{\omega,s,c}\right)$$

with $\omega_{i,s,c,c} = 0$. This formulation assumes that i) $\varrho_{\omega,s}$ is common to all individuals of the same education level s (it does not depend on c nor t); ii) $\sigma^2_{\omega,s,c}$ is common to all individuals of the same education level s and birth year cohort c (it does not depend on t), iii) all individuals are born with the same level of idiosyncratic productivity. We have

$$Var\left(\omega_{i,s,c,c}\right), \quad \text{and} \quad Var\left(\omega_{i,s,c,t}\right) = \varrho^2_{\omega,s} Var\left(\omega_{i,s,c,t-1}\right) + \sigma^2_{\omega,s,c},$$
$$\text{and} \quad Cov\left(\omega_{i,s,c,t}, \omega_{i,s,c,t+k}\right) = \varrho^k_{\omega,s} Var\left(\omega_{i,s,c,t}\right).$$

Define $\zeta_{s,c,t,k} := Cov\left(\omega_{i,s,c,t}, \omega_{i,s,c,t+k}\right)$. Observe that

$$\frac{\zeta_{s,c,t,4} - \zeta_{s,c,t,3}}{\zeta_{s,c,t,2} - \zeta_{s,c,t,1}} = \frac{\varrho^4_{\omega,s} Var\left(\omega_{i,s,c,t}\right) - \varrho^3_{\omega,s} Var\left(\omega_{i,s,c,t}\right)}{\varrho^2_{\omega,s} Var\left(\omega_{i,s,c,t}\right) - \varrho^1_{\omega,s} Var\left(\omega_{i,s,c,t}\right)} = \frac{\varrho^4_{\omega,s} - \varrho^3_{\omega,s}}{\varrho^2_{\omega,s} - \varrho^1_{\omega,s}} = \varrho_{\omega,s}.$$

Moreover,

$$Var\left(\omega_{i,s,c,c+1}\right) = \sigma^2_{\omega,s,c}.$$

These two moments moments pin down $\left(\varrho_{\omega,s}, \sigma^2_{\omega,s,c}\right)$. In our estimation we use all available moments (variances and covariances). We follow Guvenen (2009) and minimize the "distance" between the elements of the empirical covariance matrix of income residuals ω and its counterpart with the entries described above. We group households of each education level into 5-year bins by their birth year and restrict $\sigma^2_{\omega,s,c}$ to be the same for each bin. For example, households in which the head was born in years 1936, 1937, 1938, 1939 and 1940 have the same $\sigma^2_{\omega,s,c} = \sigma^2_{\omega,s,1936}$. We calculate empirical moments using all available observations and use an identity matrix in the estimation.

We present the results of our estimation in Figure B.5.

Figure B.5: Variances of idiosyncratic productivity shocks

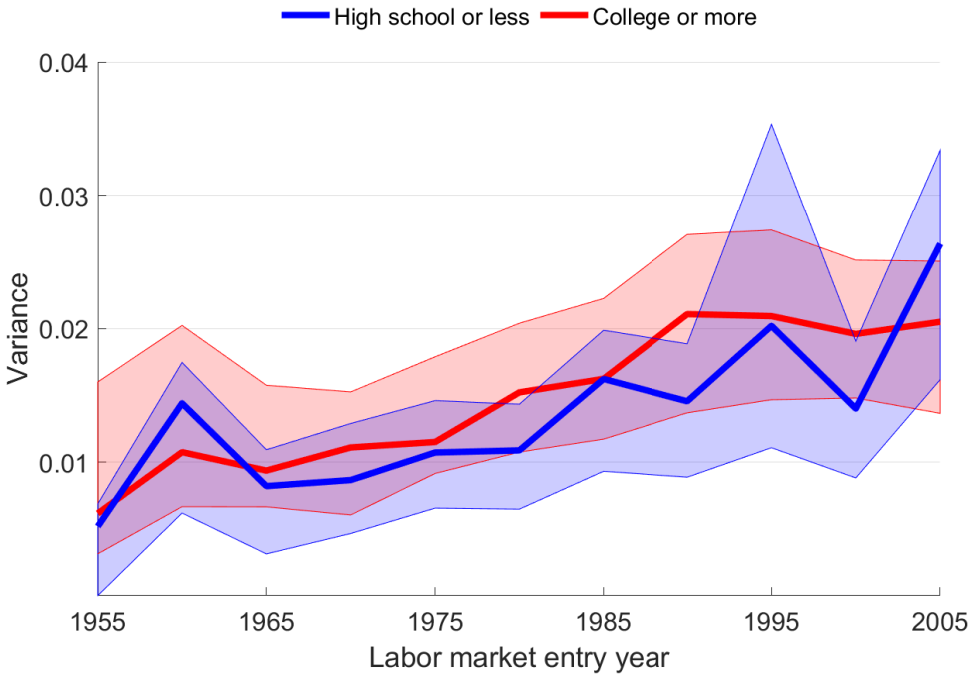

Note: Variances of idiosyncratic productivity shocks. Solid lines are point estimates, shaded areas are 95% confidence intervals (bootstrap with 1000 repetitions).

Recall that one period in the model corresponds to five years. To map the estimates to the model inputs $\bar{\varrho}_{\omega,s}, \bar{\sigma}^2_{\omega,s,c}$ we calculate

$$\bar{\varrho}_{\omega,s} = \varrho^5_{\omega,s} \quad \text{and} \quad \bar{\sigma}^2_{\omega,s,c} = \sigma^2_{\omega,s,c} \frac{1-\varrho^{10}_{\omega,s}}{1-\varrho^2_{\omega,s}}.$$

We then correct the mean of idiosyncratic income shocks $\varepsilon_{\omega,i,s,c,t}$ so that $E\left[\exp \omega_{i,s,c,t}\right] = 1$. Finally, to use the estimates process as an input in the model, we approximate each resulting AR(1) process with a 5-state Markov chain by the Rouwenhorst method. We assume the Markov chains for cohorts that entered the labor market before 1955 are the same as for the cohort that entered the labor market in 1955. Similarly, for cohorts that entered the labor market after 2005 we use the estimates for the cohort that entered the labor market in 2005.

Extra income state We add an extra income state to capture business income. This state can be reached only from the 5th state and upon exiting it the household moves to the state corresponding to the average productivity (3rd state for its education level). We assume that the transition probabilities from and to this extra state are the same for each education level s.

We use households labeled as "superstars" in the PSID data to pin down these two transition probabilities. In each 5-year period, we calculate the share of "superstars" in the population. The average share is 5.3% in our 1970-2020 sample. We also calculate the exit rate, the fraction of "superstars" that transition out of being "superstars" in the next 5-year period. The average exit rate is approximately 2%.

We assume that idiosyncratic productivity corresponding to this state is a multiple of the level of productivity associated with the 5th state, the same number for all s, j, t. PSID reports unincorporated business income for husband and wife, but the aggregate share of this income in total household labor income for households aged 25-65 amounts to roughly 13%, whereas it is 21% in the NIPA. Instead of relying on self-reported business incomes in PSID to calibrate the multiple by matching the average share of household business income in total disposable income from BEA in the years 1950-2020, equal to 21%.

B.3 Idiosyncratic return risk

To calculate the standard deviation of return shocks, we take data on share of wealth held by a particular wealth percentile group from Distributional Financial Accounts (DFAs) provided by the Federal Reserve Board. The DFAs use the Financial Accounts of the United States and the Survey of Consumer Finances (SCF). The DFAs track the evolution of share of U.S. household wealth held by five percentile groups of wealth: the top 0.1 percent, the remaining 0.9 percent of the top 1, the next 9 percent (i.e., 90th to 99th percentile), the next 40 percent (50th to 90th percentile), and the bottom half (below the 50th percentile). We combine together shares held by the top 0.1% and the next 0.9%. We average shares held by the resulting four percentile groups over the period 1989-2022: $\varpi_{\text{group}} \in \{\varpi_{0-50}, \varpi_{50-90}, \varpi_{90-99}, \varpi_{99-100}\}$.

The wealth percentiles analyzed in Hubmer et al. (2021) (HKS) differ from those in the DFAs. We use the following mapping:

1. For bottom 50% (DFAs) we assume standard deviation of 0.023 (corresponding to P0-P40 in HKS);

2. For 50-90% (DFAs) we assume standard deviation of SD of 0.081 (corresponding to P50-P60 in HKS);

3. For 90-99% (DFAs) we assume standard deviation of SD of 0.094 (corresponding to P90-P95 in HKS);

4. For 99-100% (DFAs) we assume standard deviation of SD of 0.119 (corresponding to P99-P99.5 in HKS).

We then calculate the variance of annual excess returns as

$$\varpi^2_{0-50} \cdot \sigma^2_{r,0-50} + \varpi^2_{50-90} \cdot \sigma^2_{r,50-9} + \varpi^2_{90-99} \cdot \sigma^2_{r,90-99} + \varpi^2_{99-100} \cdot \sigma^2_{r,\text{99-100}}.$$

One period in the model corresponds to five years. For simplicity, we approximate the variance of five-year returns as 5 times the variance of annual returns. This approximation is exact if the deterministic part of returns is equal to zero.

B.4 Production function

We use Penn World Tables 10, published by the Groningen Growth and Development Center (GGDC), to calibrate all the time-varying parameters of the production function. Below we describe the details of processing the GGDC data as well as extrapolation. We remove the cyclical component by applying the Hodrick-Prescott filter. The values for each period are obtained as five-year averages of the trend component.

Depreciation rates d_t (Figure B.6a, variable `delta`) We take annual depreciation rates and aggregate them to five-year rates.[15] The trend component of depreciation grows from roughly 15% over a five-year period to roughly 21%. Since the trend component did not exhibit much change in the 1960s, we assume a constant level in the years 1935-1955, equal to the trend component of the depreciation rate in 1955.

Output elasticities with respect to labor $1 - \alpha_t$ (Figure B.6b, variable `labsh`). Labor share in our model is equal to $1 - \alpha_t$ matched directly labor share in the U.S. in 1950-2019. We assume the trend component of the labor share declined linearly between 1935 and 1950 (there is no data for these years in PWT 10). We assume that labor share declines from 59.7% in 2020 to 57% in 2100, with the rate of decline gradually slowing down, as portrayed in Figure B.6b.

Labor-augmenting technological progress γ^A_{t+1} (Figure B.6c, variable `rtfpna`) We take raw TFP growth estimates from PWT 10 to calculate the TFP level (normalizing TFP in 1935 to one). Next, we adjust it using α_t to make it labor-augmenting. We then divide the resulting measure of labor-augmenting productivity by a time-varying factor that represents productivity changes resulting from changing age and education composition, and changing skill premium. This procedure yields a path of A_t that starts in the 1950s and ends in 2017 which we use in all demographic scenarios considered in this paper. For the years between 1930 and 1950 we assume flat TFP growth rate. For the years after 2020 we take the estimates of 0.6% *per annum*, consistent with Fernald (2016) who projects future annual overall TFP growth rates between 0.4% and 0.8%.

[15] The source of variation in depreciation rates is the changing composition of the U.S. capital stock: GDDC does not adjust depreciation rates over time for the same type of capital input, but it computes capital input shares, which serves to provide a weighted average depreciation rate for the U.S. economy.

Figure B.6: Technology

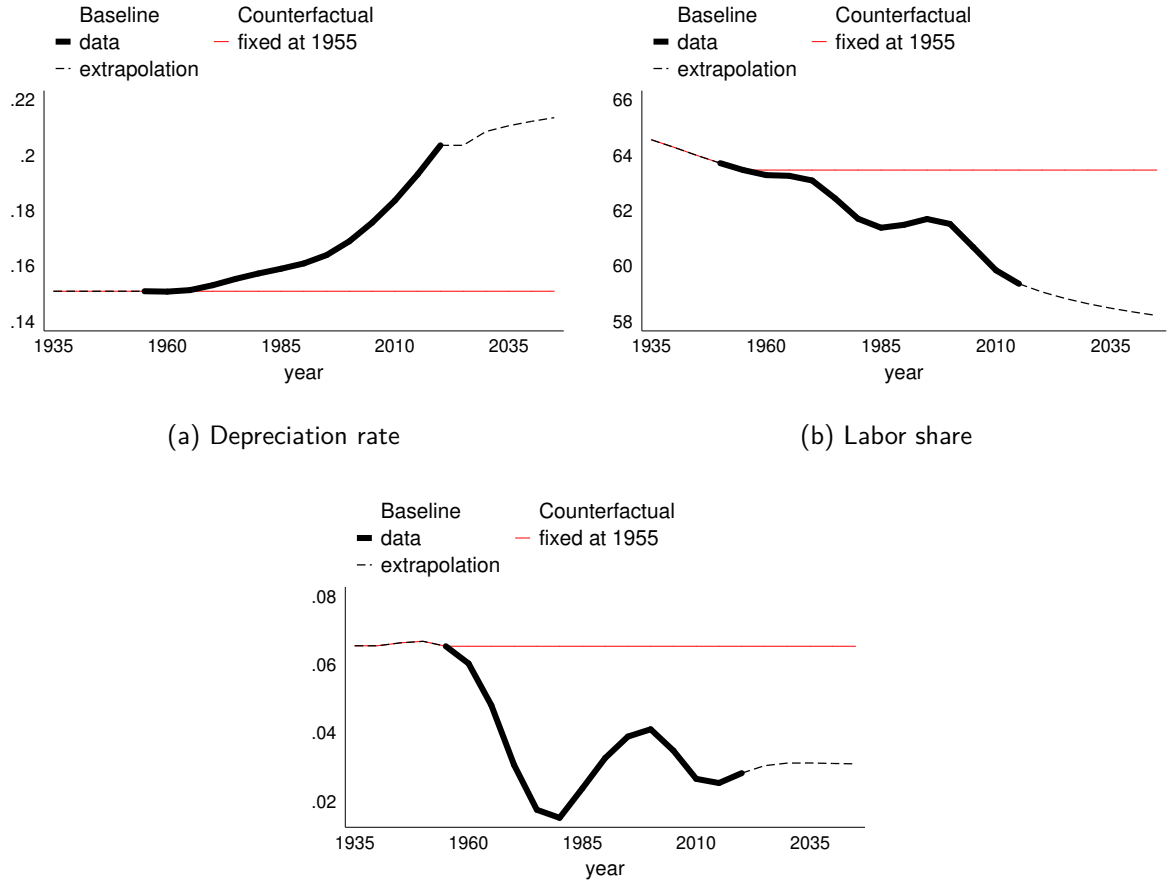

(a) Depreciation rate

(b) Labor share

(c) TFP growth rate

Note: Data are taken from Penn World Tables 10. Depreciation rate is variable `delta`, labor share is variable `labsh`, TFP growth rate is variable `rtfpna`. The data was adjusted to five-year periods. We also remove the cyclical component by applying Hodrick-Prescott filter. The values for each period are obtained as five-year averages of the trend component.

B.5 Taxes

Average tax rates on labor income $\tau_{\ell,t}$, capital income $\tau_{k,t}$, and consumption $\tau_{c,t}$ (Figures B.7a, B.7b, B.7c). Tax rates constitute inputs into model directly, in other words, there is no smoothing of tax rates. Extrapolation takes the last data point and assumes the taxes constant into the future. As described in the A.3, we close the model with government expenses.

We use series from McDaniel (2007) to calibrate the average labor income tax rate $\tau_{\ell,t}$, the gross capital income tax rate $\tau_{k,t}$, and the consumption tax rate $\tau_{c,t}$. These rates match the shares of revenues from capital income tax, labor income tax, and consumption tax observed in the data. We calculate the five-year averages of the series to use as inputs for our model. In the early periods, for which we do not have data, we assume the tax rates are equal to their first available value of the five-year average. We assume that tax rates in the future are equal to their last observed value of the five-year average.

Labor income tax progressivity λ_t (Figure B.7d). To obtain λ_t, the parameter governing the extent of labor income tax progressivity, we follow Ferrere and Navarro (2018). They calculate $\lambda_t = (AMTR_t - ATR_t) / (1 - ATR_t)$, where $AMTR_r$ is the average marginal tax rate and ATR_t

Figure B.7: Tax rates

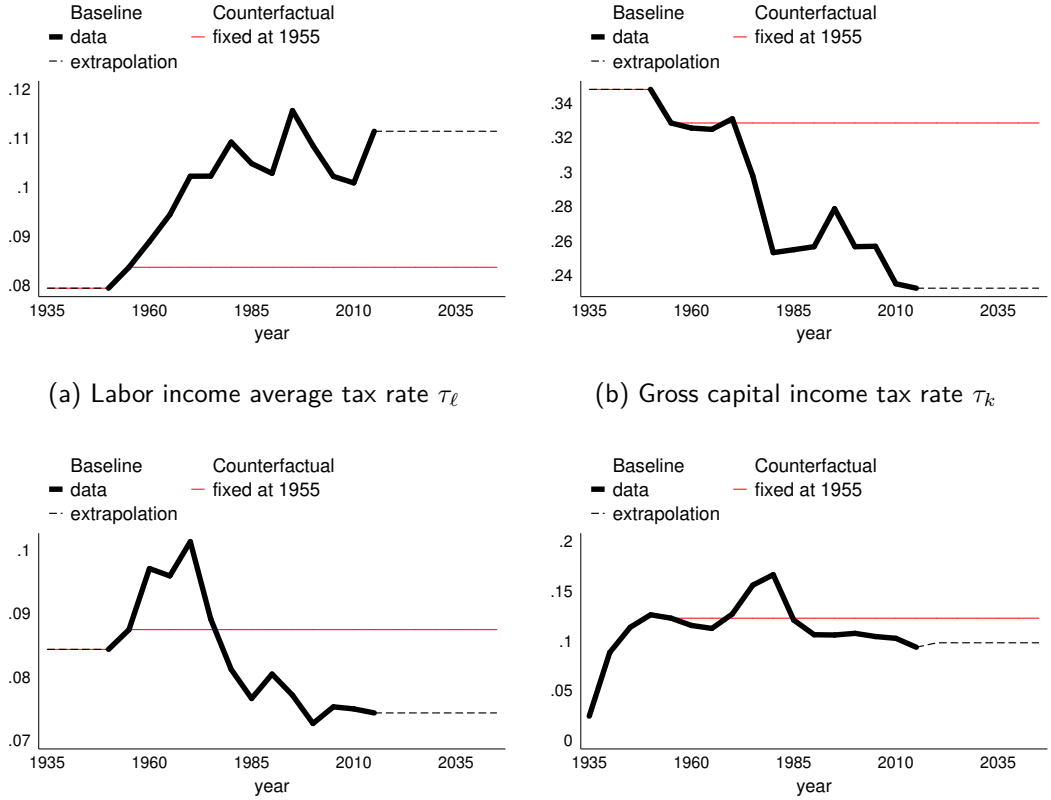

(a) Labor income average tax rate τ_ℓ

(b) Gross capital income tax rate τ_k

(c) Consumption tax rate τ_c

(d) Labor income tax progressivity, λ

Note: labor income tax average rate, gross capital income tax rate, and consumption tax rate are from McDaniel (2007). Labor income tax progressivity, λ, is calculated by using measures of average marginal tax rates from Barro and Sahasakul (1983) and Mertens and Montiel Olea (2018) and total market income from Piketty and Saez (2003). See the main text.

is the average tax rate. We use measures of $AMTR_t$ from Barro and Sahasakul (1983) for 1916-1946 and from Mertens and Montiel Olea (2018) since 1946. Average tax rates are calculated as the sum of federal personal current taxes divided by the total market income from Piketty and Saez (2003). We calculate the five-year averages of the resulting series to use as input for our model.

B.6 Social security contributions

To set the effective rate of social security contribution $\tau_{ss,t}$ we use data on social security contributions relative to GDP from the OECD and calculate the five-year averages. See Figure B.8 for the path that we use as an input. We assume the ratio is constant after 2015, consistent with its relative stability since the 1990s. We assume the ratio was low in the 1940s and that this ratio gradually increased in the 1950s and the 1960s.

The parameters used to calculate pensions in the social security system, including the OASDI cap and the bend-points for AIME ($F_{1,t}, F_{2,t}$) are taken from McGrattan and Prescott (2017) and remain constant over time.

We use the parameter $\varrho_{\bar{j},t}$ to adjust the generosity of pension benefits (see Section A.1). In the early period of our model, social security coverage was not universal (the 1935 Act provided compulsory coverage for workers in commerce and industry only, by 1956 the coverage was extended

Figure B.8: Social security contributions to GDP

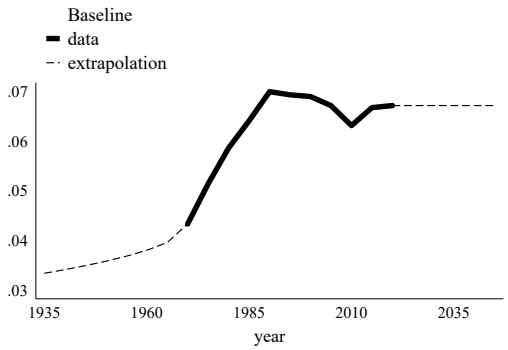

Note: Social security contributions to GDP series is from OECD. Social security contributions are calculated as the sum of contributions, voluntary contributions, and imputed contributions. Data are adjusted to adjusted to five-year periods by calculating five-year averages.

to approximately 90% workers). In addition, there were very few retirees given the recent adoption of social security. Over subsequent years, coverage increased, and data became informative of the actual share of beneficiaries in society. We manipulate $\varrho^{-}_{\bar{j},t}$ to capture these patterns and calibrate its value so that the ratio of benefits to GDP in our model aligns closely with the data (see Figure D.3). Figure B.9 portrays the time evolution of $\varrho^{-}_{\bar{j},t}$. We use the same path in all our experiments.

We do not explicitly introduce Medicare in our framework. In our model, Medicare is included as a part of government purchases (once it is introduced) financed by tax revenue consistent with the data. In other words, Medicare is included on the macroeconomic level. In addition, our model does not feature health shocks. This has important consequences. On the one hand, there are no precautionary savings to insure against the health shocks in the behavior of the agents in our model. On the other hand, introducing explicit Medicare transfers and assigning them to individuals would not introduce any interesting patterns in saving behavior.

Introducing health shocks and Medicare could further amplify the effect of rising longevity on wealth inequality. In our model, the agents save for old-age consumption, and the longer they expect to live in retirement, the higher the optimal accumulated stock of savings. If rising longevity after retirement was associated with an increased risk of adverse health shocks, the old-age saving motive would be stronger than in a model without health shocks. Medicare operates as an insurance mechanism (similar to pensions), but empirical research as well as applied macroeconomic models show that the insurance is incomplete and agents save (or dis-save slower) in the old age in anticipation of out of pocket medical expenses.

Figure B.9: Replacement rate scale parameter $\varrho_{\bar{j},t}$

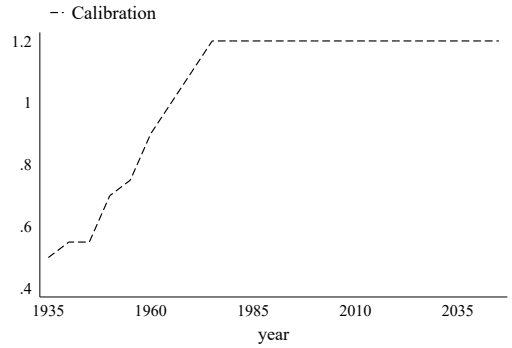

Note: The replacement rate scale parameter is calibrated to match the ratio of pension benefits to GDP. We restrict the values of this parameter to be nondecreasing over time.

C Online Appendix: population structure

Figure C.1 shows comparison of population structure in selected years in the baseline calibration and in the counterfactual scenario with longevity fixed at the 1955 levels.

Figure C.1: Population structure: a comparison for four periods

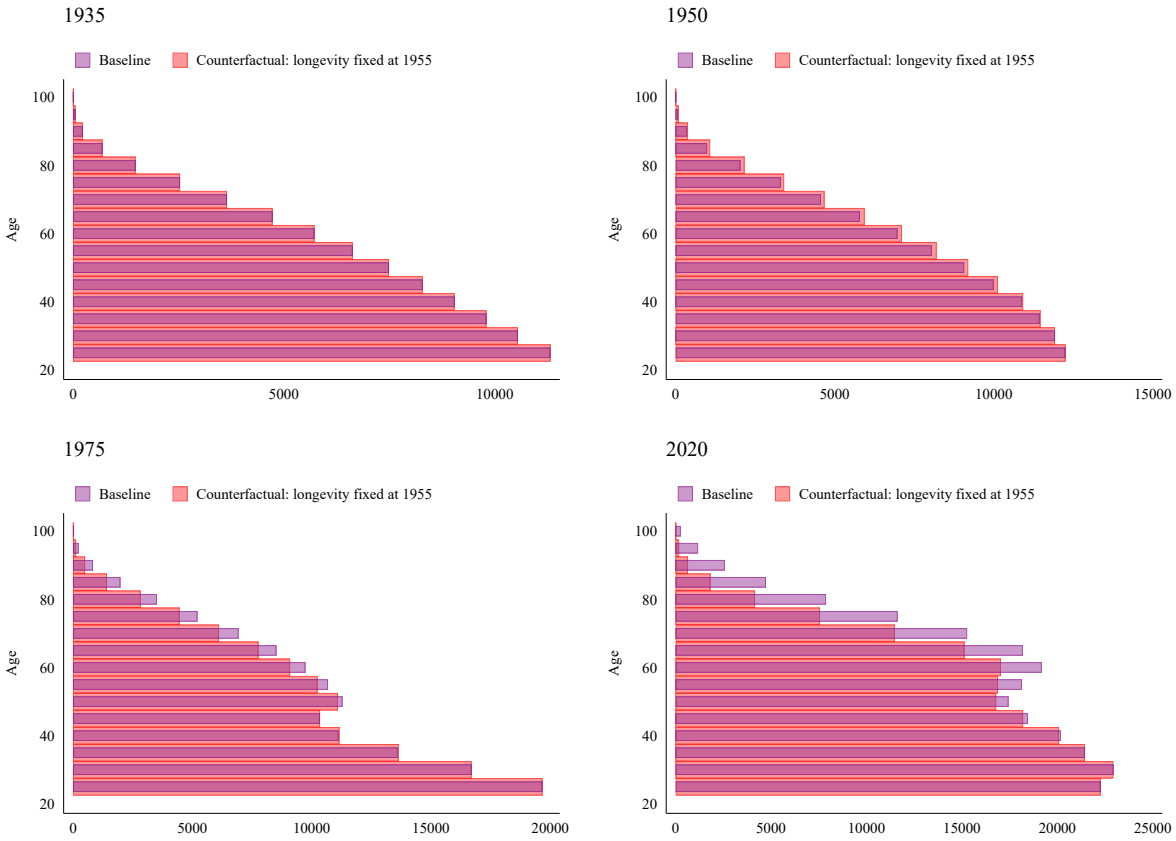

Note: data from Centers for Disease Control and Prevention (CDC).

D Online Appendix: model vs data

Virtually almost all macroeconomic parameters in the model are derived from empirical data. The model includes four key endogenous variables: (1) the rate of return, r_t; (2) average hours worked per capita; (3) the expenditure on social security benefits as a share of GDP; and (4) the ratio of bequests to GDP.

We begin by comparing the rate of return r_t in the model to data from PWT 10, shown in Figure D.1. The model is calibrated to match the initial interest rate value for the 1950s, after which its behavior is fully endogenous. The model successfully replicates the overall trend and captures some degree of fluctuations over time. The discrepancy between the model and the data in recent years could stem from the absence of government debt in the model. In the data, government debt has increased significantly in recent years, which likely mitigated the decline in interest rates observed in the real economy. In our model, government expenses serve as the fiscal closure mechanism, but public debt is excluded to avoid introducing ad hoc assumptions in counterfactual scenarios. As a result, the increased savings in the model generate a stronger "saving glut" mechanism compared to the data, leading to a slightly steeper decline in the interest rate.

Figure D.1: The real interest rate, model vs data

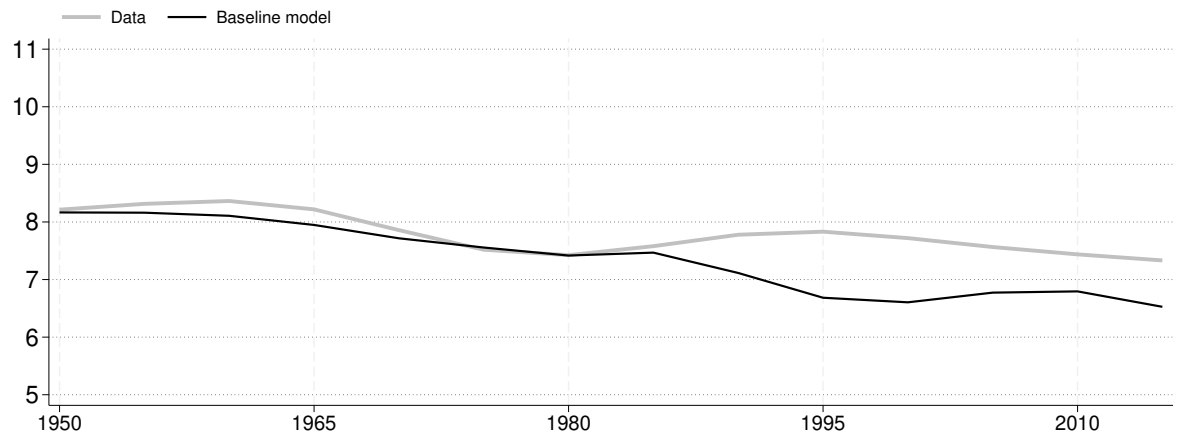

Note: The thick gray line represents data from Penn World Tables 10 (variable `irr`), adjusted to five-year periods by applying a Hodrick-Prescott filter with a parameter of 6.25 and calculating five-year averages of the trend component, then converted to an annual rate of return. The solid black line represents the annual rate of return r_t from our baseline simulation.

Next, Figure D.2 compares average annual hours in the model to the data. Following Boppart and Krusell (2020), we calculate average hours in the data by multiplying average hours worked per engaged person by the number of engaged persons (from Penn World Tables 10) and dividing by the population aged 20–64 (from the OECD). Both the data and model values are normalized to their means for comparability.

The model accurately captures the lack of a long-term trend in average hours in the postwar U.S., consistent with Boppart and Krusell (2020). However, the model generates slightly larger fluctuations than observed. The largest discrepancy occurs after 2010, as the model does not replicate the decline in hours associated with the Great Recession.

Figure D.2: Average annual hours per capita aged 20–64, model vs data

Note: The thick gray line represents the data, first adjusted to five-year periods by applying Hodrick-Prescott filter with parameter 6.25 and calculating five-year averages of the trend component), and then normalized by dividing by the 1950-2015 average of the trend component. To obtain average annual hours per capita aged 20-64 in the data we follow Boppart and Krusell (2020). We multiply the average annual hours worked by person engaged (variable `avh`) by the number of persons engaged (variable `emp`) from Penn World Tables 10 and divide by population aged 20-64 from the OECD. The solid black line represents the rate of average hours worked in the model, normalized by the 1950-2015 average.

For social security, we calibrate the model using the ratio of social security contributions to GDP. Since our steady state is calibrated to 1935, when social security coverage was limited, we introduce an additional parameter, $\varrho^{-}_{\bar{j},t}$ (see Section A.1), to capture the expansion of coverage over time.[16] The path of $\varrho^{-}_{\bar{j},t}$ is shown in Figure B.9 in Online Appendix B.6. Figure D.3 shows that the model replicates both the levels and time variation of social security expenditures well. Furthermore, the model's future projections align closely with those of the Congressional Budget Office.

[16] Note that $\varrho^{-}_{\bar{j},t}$ alone does not determine the share of social security expenditures in GDP; this share is endogenously determined in the model equilibrium.

Figure D.3: Share of expenditure on social security benefits in GDP, model vs data

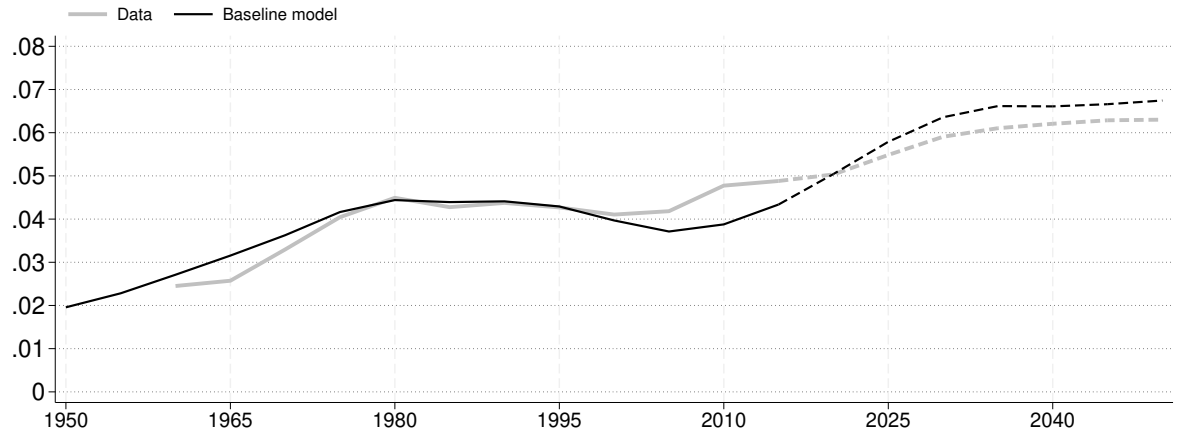

Note: The solid gray line represents data from the Congressional Budget Office (`SS.PGDP` variable), with the forecast as of 2015 shown by the gray dashed line. To smooth the series, we apply the Hodrick-Prescott filter and calculate five-year averages of the trend component. The solid black line shows the model's baseline scenario for years prior to 2015, while the dashed black line represents the model's projections for years after 2015.

Finally, we compare the ratio of bequests to GDP in the model with data. In our model, bequests are purely accidental, determined by mortality and wealth holdings, with no extra parameters to influence them. Hendricks (2001) estimate aggregate inheritances at 1.2–2% of GNP, while Alvaredo et al. (2017) report a slight decline in annual inheritance flows from 8% of GDP in the 1950s to 7% after 2000 (see their Figure A3). In comparison, our model predicts bequest flows of 5.5% in the 1950s and 5.2% after 2000, aligning closely with the 5% target used by Straub (2019).

We also compare our model to insights from microeconomic data, focusing first on the reliability of the income process. In Figure D.4, we present Lorenz curves generated by the model and compare them to their empirical counterparts. Each model period represents five years, and two consecutive periods of model-generated data are combined to approximate the decades of the 1970s, 1980s, 1990s, 2000s, and 2010s. For the empirical counterparts, we use PSID data, combining all observations within each decade to increase sample sizes.

To ensure consistency with the model, we restrict the data sample to individuals aged 20–65 and exclude observations with negative reported incomes, as such cases are ruled out by our income process. As shown in Figure D.4, the model replicates the income distribution in the data quite well. While income shocks and life-cycle patterns were estimated from the PSID, other features of the income process, such as the college premium and college shares, were sourced from external datasets. Thus, the model's ability to match the income distributions in the data, despite this not being a direct calibration target, is particularly reassuring.

Finally, we compare the role of demographics in the Survey of Consumer Finances (SCF) data to the magnitudes implied by our model.[17] Bauluz and Meyer (2024) utilize the same data to study saving rates, measured as the ratio of assets to income, across birth cohorts as they age. Their findings indicate that successive birth cohorts tend to exhibit higher saving rates, which aligns well with the insights generated by our model.

To further evaluate the match between our model and the data, we decompose a measure of wealth inequality into between-cohort and within-cohort components. While the Gini coefficient does not allow for such a decomposition, the Generalized Entropy (GE) index does. GE measures take the

[17] We use the extended sample provided by Kuhn et al. (2020a).

Figure D.4: Lorenz curves of income distribution: data vs. model

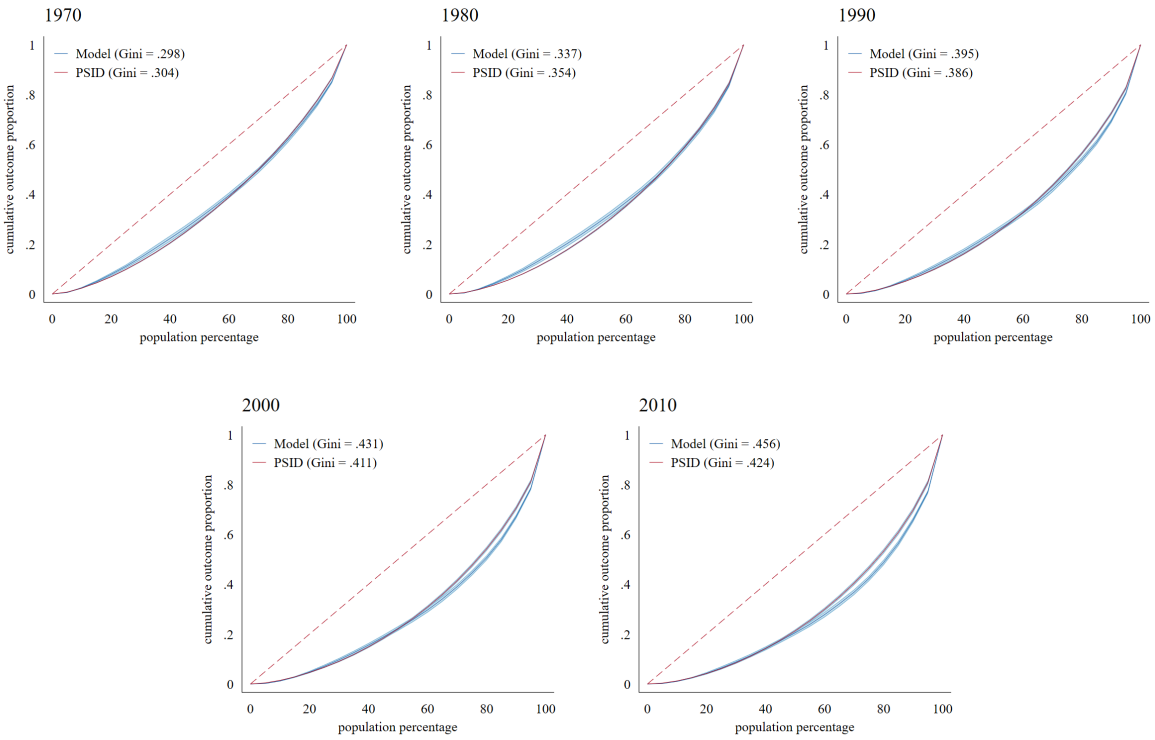

Note: Labor income data are sourced from the PSID, with population weights applied to the PSID data. In the model, probability mass serves as weights. Both datasets are restricted to individuals aged 20–65 to align with the model. For clarity, "superstars" are excluded from both the model and the data.

following form:

$$\begin{aligned} GE(\iota) &= GE_b(\iota) + GE_w(\iota) \\ GE_{between}(\iota) &= \frac{1}{(\iota^2 - \iota)} \left[\sum_{j=1}^{J} n_j \cdot \left(\frac{\overline{a_j}}{\overline{a}} \right)^{\iota} - 1 \right] \\ GE_{within}(\iota) &= \sum_{j=1}^{J} GE_j(\iota) \cdot n_j \cdot \left(\frac{\overline{a_j}}{\overline{a}} \right)^{\iota}, \end{aligned}$$

where $j = 1, ..., J$ denotes birth cohorts, $\iota \notin \{0, 1\}$[18] is a parameter that governs the sensitivity of GE measure, a denotes assets (with $\overline{a}$ representing average assets in the economy and $\overline{a_j}$ representing average assets of birth cohort j), and n_j denotes the share of birth cohort j. By design, the GE measure allows for decomposition $\Delta GE(\iota) = \Delta GE_b(\iota) + \Delta GE_w(\iota)$, where the change in overall inequality is the sum of changes in between-cohort $\Delta GE_b(\iota)$ and nd within-cohort $\Delta GE_w(\iota)$ inequality.

Not only is the GE index decomposable, but Lewandowski et al. (2024) also demonstrate that for $\iota = 0.5$, the GE index closely replicates the dynamics of the Gini coefficient. Importantly, the main conclusions regarding the decomposition into between- and within-cohort inequality remain robust to the choice of this parameter.

We decompose changes in wealth inequality in both the model and the data into two components: the between-cohort component (ΔGE_b) and the within-cohort component (ΔGE_w). The results are presented in Figure D.5, where we display side-by-side bars for a given period, comparing the data and the model. Gray bars represent the data, while purple bars represent the model, with darker shades indicating the between-cohort contribution and lighter shades indicating the within-cohort contribution.

Although these patterns were not explicitly targeted in the calibration, our model accurately captures the evolving nature of the between- and within-cohort contributions to changes in wealth inequality. While the magnitudes observed in the data are larger than those in the model, the patterns generated by the model align remarkably well with the empirical regularities.

[18] The GE index for $\iota = 0$ simplifies to the mean-log deviation, and for $\iota = 1$, it becomes a Theil index.

Figure D.5: The contribution of between-cohort inequality and within-cohort inequality to change in overall inequality

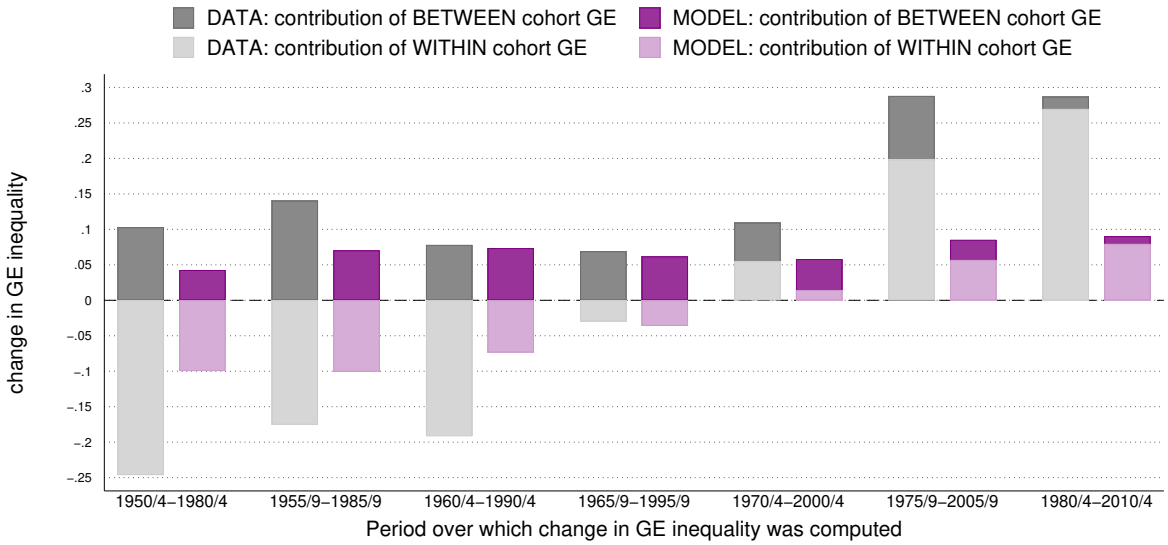

Note: We obtain household wealth data, measured as net assets, from the Survey of Consumer Finances (SCF) extended sample (Kuhn et al., 2020a). Observations with negative assets were excluded from the SCF sample, as the model imposes a non-negativity constraint on asset accumulation. Population weights were applied to the SCF data, while probability mass served as weights in the model data. Both datasets were censored at the 99th percentile for consistency. To measure wealth inequality, we use the Generalized Entropy (GE) index with $\iota = 0.5$, as it closely replicates the time variation observed in the Gini coefficient of wealth inequality.

Our decomposition of changes in wealth inequality into between- and within-cohort components does not directly correspond to the endogenous processes in the model. It is important to note that rising longevity can influence both components. The between-cohort component reflects the fact that birth cohorts with differing life expectancies after retirement accumulate varying levels of wealth by the time they retire. Meanwhile, the within-cohort component captures the extent to which agents within the same cohort respond similarly to the old-age saving motive driven by increased longevity.

Additionally, the dynamics of rising longevity involve the exit of older cohorts and the entry of new ones, a mechanism similar to the entries and exits in top wealth shares modeled by Gomez (2023). A comprehensive account of demographic processes in the data is provided by Lewandowski et al. (2024).

E Online Appendix: results

In the main text, we focus on the impact of demographic factors on wealth inequality, as this represents our main contribution to the literature, and we examine in detail how they influence its evolution. For comparison, we also analyze the total effects of other factors, such as incomes, taxes, and technology. However, due to space limitations, we could not provide a more in-depth analysis of these factors in the main text. Instead, we offer a more detailed examination of them here.

E.1 Incomes and evolution of wealth inequality

Between 1950 and 2015, incomes underwent significant changes, characterized by three key developments. First, the share of college graduates increased, shown in Figure B.1. This shift can influence income and wealth inequality in either direction: it can reduce inequality by narrowing the gap in educational attainment and increasing opportunities, or it can exacerbate inequality, especially, if the benefits of higher education are large.

Second, the college premium rose (see Figure B.3), which likely amplified income and wealth inequalities by increasing the earnings gap between college graduates and those without a college education. However, it may also have contributed to boosting the wealth of the middle class, potentially reducing wealth inequality.

Third, income risk increased for both college graduates and individuals with less than a college education as shown in Figure B.5. This had two opposing effects: on the one hand, greater income dispersion led to more dispersed wealth, increasing wealth inequality; on the other hand, heightened income risk incentivized individuals to save more due to precautionary motives, particularly among those with fewer assets, which helped reduce wealth inequality.

The net effect of these three factors on the wealth Gini coefficient is ultimately a quantitative question. Figure D.4 illustrates how income inequality evolved over time in both our model and the data. Our model effectively replicates the observed increase in the income Gini coefficient.

To quantify the effect of income changes on wealth inequality, we conduct a counterfactual scenario in which the college premium and the share of college graduates are fixed at their 1955 levels, while income risk is held constant at its initial level. Figure E.1, constructed in a similar fashion as Figure 3, illustrates the contribution of income changes to the evolution of the Gini coefficient between 1950 and the years 1975, 2015, and 2050.

Our findings show that income changes have significantly contributed to the increase in the wealth Gini coefficient. By 1975, the coefficient was 1.2 Gini points higher due to income changes. This upward trend persisted, with the Gini coefficient rising by 2.9 points by 2015. By 2050, income changes are projected to account for an increase of 3.7 Gini points.

Figure E.1: Impact of evolution of income determinants on wealth inequality (in Gini points)

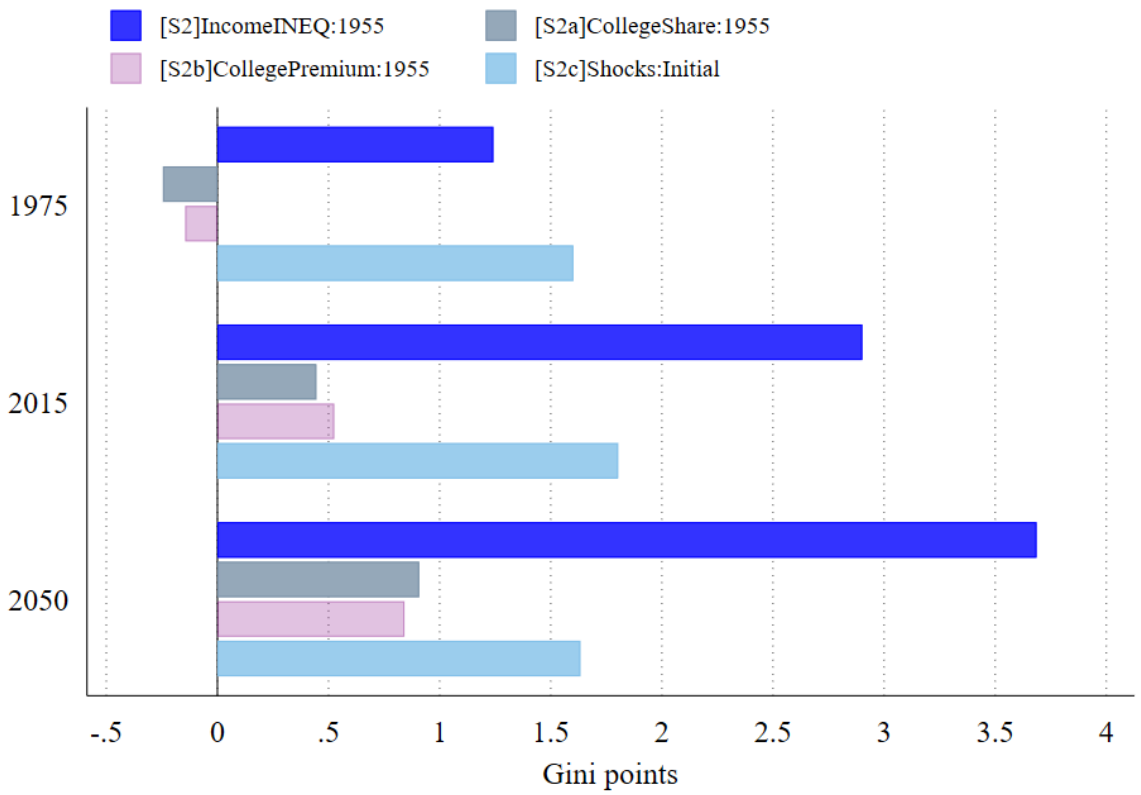

Note: The bars depict the differences in the wealth Gini coefficient for a given year between the baseline scenario and the respective counterfactual scenarios $\Delta_t = \boldsymbol{G}_t^b - \boldsymbol{G}_t^c$. A positive number indicates that a given factor contributed to the increase in the Gini coefficient, while a negative value indicates a decrease. Counterfactual scenario [S2]IncomeINEQ:1955 was computed by fixing income characteristics at their 1955 levels (see Figures B.1, B.3 and B.5), while keeping all other aspects as in the full model. Counterfactual scenario [S2a]CollegeShare:1955 was computed by fixing the college share in the population to its 1955 level (see Figure B.1), while keeping the rest as in the full model. Counterfactual scenario [S2b]CollegePremium:1955 was computed by fixing the college premium to its 1955 level (see Figure B.3), with all other factors remaining consistent with the full model. The counterfactual scenario [S2c]Shocks:Initial is computed by fixing the parameters of the stochastic process governing the idiosyncratic component of income at their initial levels (corresponding to the cohort entering the labor market in 1955, see Figure B.5 in section B.2), while keeping all other elements consistent with the full model.

Next, Figure E.1 illustrates how the three aforementioned factors contribute to these developments.

1. Scenario [S2a]: The increase in the share of college graduates reduces wealth inequality by 0.2 Gini points in 1975 but leads to increases of 0.4 and 0.9 points in 2015 and 2050, respectively.

2. Scenario [S2b]: The rise in the college premium slightly reduces wealth inequality by less than 0.1 Gini points in 1975 but subsequently increases it by 0.5 and 0.8 Gini points in 2015 and 2050, respectively.

3. Scenario [S2c]: The increase in idiosyncratic income risk contributes to a rise in the wealth Gini coefficient by approximately 1.6 Gini points across all analyzed years.

E.2 Taxes and wealth inequality

The contribution of taxation changes to inequality is a highly debated topic. Here, we present the predictions of our model. Over the analyzed period, several changes to taxation policies occurred, as shown in Figure B.7.

First, the average income tax rate increased, which is expected to reduce both income and wealth inequality. An increase in the progressive average income tax rate lowers the post-tax income Gini coefficient, which affects the wealth Gini in two ways. On one hand, individuals with higher incomes tend to save proportionally more, so higher taxes reduce wealth inequality. On the other hand, reduced income risk decreases precautionary savings, particularly for lower-income households, which can increase wealth inequality.

Second, the consumption tax rate rose before 1975 and then declined, which can affect wealth Gini in any directions.

Third, the tax on capital income decreased, which, by encouraging savings, could theoretically either increase or decrease the wealth Gini coefficient.

Finally, the progressiveness of labor income taxation evolved over the analyzed period. While it is currently less progressive than in the 1950s, it increased prior to 1975 and declined afterward. Labor income progressivity has two opposing effects: it reduces income risk, leading to lower precautionary savings (with stronger responses from households with fewer assets) and increasing wealth inequality, but it also makes post-tax incomes more equal, which can reduce disparities in asset holdings.

Our findings indicate that tax changes have contributed to a decrease in the wealth Gini coefficient, as shown in scenario [S3]Taxes:1955 in Figure E.2, constructed in a similar fashion as Figure 3. By 1975, the coefficient was 1 Gini point lower due to these changes. This downward trend continued, with the Gini coefficient reduced by 1 Gini point by 2015. By 2050, tax changes are projected to result in a decrease of 0.8 Gini points.

Figure E.2: Impact of tax changes to the wealth inequality (in Gini points)

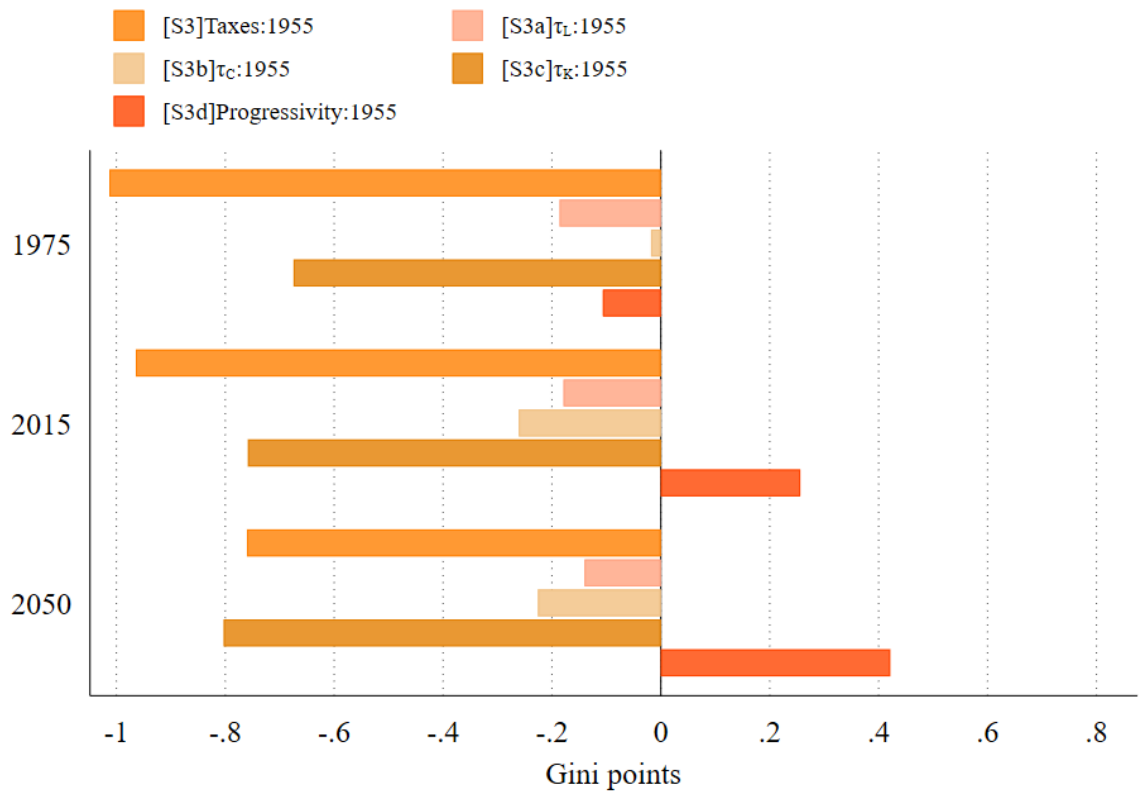

Note: The bars depict the differences in the wealth Gini coefficient for a given year between the baseline scenario and the respective counterfactual scenarios, as defined by the formula $\Delta_t = \boldsymbol{G}_t^b - \boldsymbol{G}_t^c$. A positive value indicates that a given factor contributed to an increase in the Gini coefficient, while a negative value indicates a decrease. Counterfactual scenario [S3]Taxes:1955 was computed by fixing all tax rates to their 1955 levels (see Figure B.7), while keeping all other aspects as in the full model. Counterfactual scenario [S3a]τ_L:1955 was computed by fixing only the average labor income tax rate (τ_ℓ) to its 1955 level, while the rest of the model remained unchanged. Counterfactual scenario [S3b]τ_C:1955 was computed by fixing only the consumption tax rate τ_c to its 1955 level, with all other elements of the model unchanged. Counterfactual scenario [S3c]τ_K:1955 was computed by fixing only the capital income tax rate (τ_K) to its 1955 level, leaving the rest of the model consistent with the full model. Counterfactual scenario [S3d]Progression:1955 was computed by fixing the degree of progressiveness in the labor tax (λ) to its 1955 level, while all other aspects remained as in the full model.

Next, Figure E.2 illustrates how the four mentioned above factors contribute to these developments.

1. Scenario [S3a]τ_L:1955: The increase in the average labor income tax rate reduces wealth inequality by 0.2 Gini points in 1975 and continues to have a mitigating effect over time. By 2015 and 2050, the Gini coefficient is lower by 0.2 and 0.1 Gini points, respectively.

2. Scenario [S3b]τ_C:1955: The increase in consumption tax contributed to a slight reduction in wealth inequality, decreasing the Gini coefficient by 0.01, 0.3 and 0.2 Gini points in 1975, 2015, and 2050, respectively.

3. Scenario [S3c]τ_K:1955: The decline in tax on capital income reduces wealth inequality, lowering the Gini coefficient by 0.7, 0.8, and 0.8 Gini points in 1975, 2015, and 2050, respectively.

4. Scenario [S3d]Progressivity:1955: The initial increase in labor tax progressivity lowers the

Gini coefficient by 0.1 Gini points in 1975. However, as labor taxes become less progressive, aftwerward, wealth inequality rises, with the Gini coefficient increasing by 0.3 Gini points by 2015 and projected to rise by 0.4 Gini points by 2050.

E.3 Technology and wealth inequality

Between 1950 and 2015, parameters describing technology underwent significant changes, characterized by three key developments, see Figure B.6. First, the labor share declined. Although usually one expects that a decline in the labor share exacerbates wealth inequality, under specific conditions - such as broad distribution of capital income, effective redistributive policies, or increased access to capital for lower-income groups - it could result in a reduction in inequality.

Second, TFP growth slowed down. Lower TFP growth results in lower interest rates, which generally tends to reduce wealth inequality, although, theoretically, it could also increase it under certain conditions. Additionally, slower TFP growth affects the growth rate of average labor incomes over the life cycle. This can encourage younger individuals to save more, as saving for old age becomes a greater priority. This effect is likely to be more pronounced among low-income individuals. Overall, one would expect that a productivity slowdown reduces wealth inequality, although the possibility of the opposite effect cannot be entirely ruled out. Ultimately, the impact is a quantitative question.

Third, the increase in the depreciation rate lowers the interest rate which can affect wealth inequality through several interconnected mechanisms. On the one hand, wealthy individuals may see a slowdown in accumulation of their wealth. On the other hand, low rates of return may discourage savings among individuals with little assets. The overall impact depends on the specific features of the model, such as how savings, investment, and income are distributed across agents, as well as the relative importance of capital and labor income.

Our findings indicate that technological changes have contributed to a decrease in the wealth Gini coefficient, as shown in scenario [S4]Technology:1955 in Figure E.3, constructed in a similar fashion as Figure 3. By 1975, the coefficient was 0.9 Gini points lower due to these changes. This downward trend persisted, with the Gini coefficient lowered by 0.9 Gini point by 2015. By 2050, technological changes are projected to result in a decrease of 1 Gini point.

Next, Figure E.3 illustrates also how the three mentioned above factors contribute to these developments.

1. Scenario [S4a]LabShare:1955: It examines the decline in the labor share, which decreases wealth inequality by 0.9 Gini points in 1975 and continues to have mitigating effect over time. By 2015 and 2050, the Gini coefficient is reduced by 0.9 and 1.0 Gini points, respectively.

2. Scenario [S4b]TFP:1955: It consider slowdown in TFP growth, which mitigates wealth inequality. In 1975, it reduces the Gini coefficienty by 0.5 Gini points. This persist, with the Gini coefficient reductions of 0.9 and 0.5 Gini points in 2015 and 2050, respectively.

3. Scenario [S4c]Depr:1955: It assesses the impact of the decline in deprecation, which increases wealth inequality. Due to this factor, the Gini coefficient is higher by 0.1, 0.7, and 0.9 Gini points in 1975, 2015, and 2050, respectively.

Figure E.3: Impact of technological changes on wealth inequality

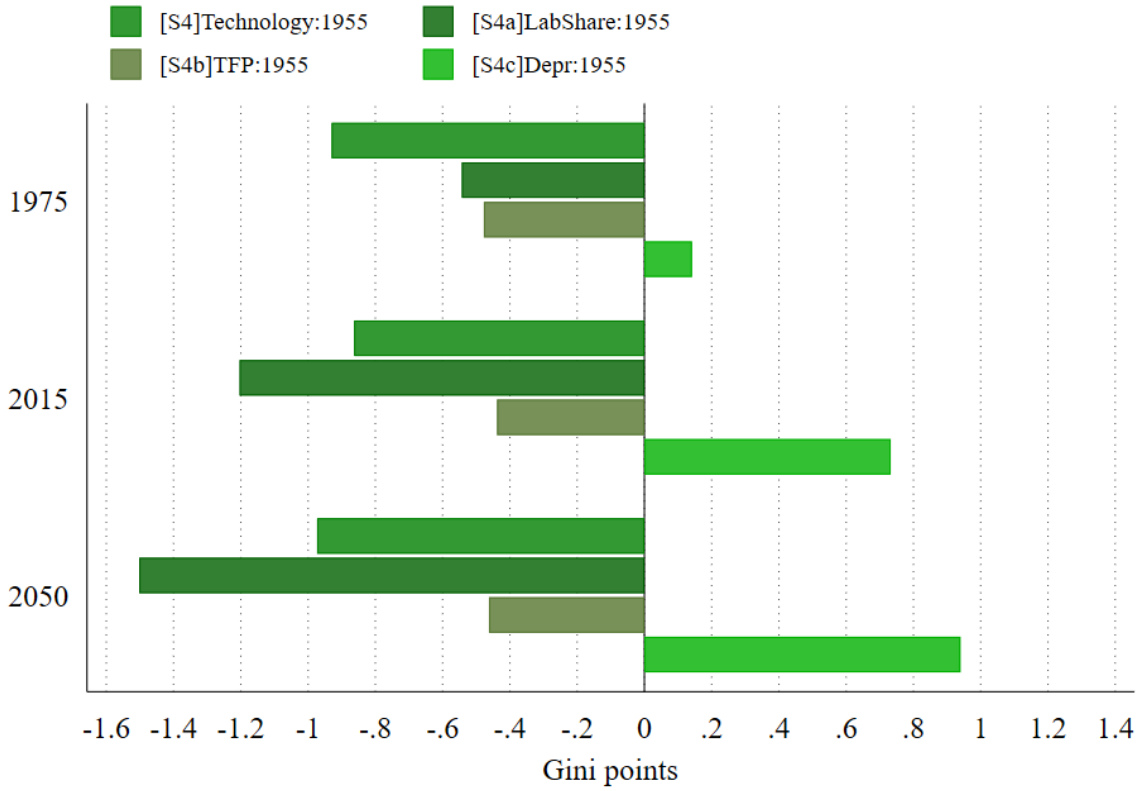

Note: The bars depict the differences in the wealth Gini coefficient for a given year between the baseline scenario and the respective counterfactual scenarios, as defined by the formula $\Delta_t = \boldsymbol{G}_t^b - \boldsymbol{G}_t^c$. A positive value indicates that a given factor contributed to an increase in the Gini coefficient, while a negative value indicates a decrease. Counterfactual scenario [S4]Technology:1955 was computed by fixing the labor share, the growth rate of technology, and the depreciation rate to their 1955 levels (see Figure B.6), while keeping all other aspects as in the full model. Counterfactual scenario [S4a]LabShare:1955 was computed by fixing only the labor share (α_t) to its 1955 level, while the rest of the model remaining unchanged. Counterfactual scenario [S4b]TFP:1955 was computed by fixing only the TFP growth rate (γ_t^A) to its 1955 level, with all other elements of the model left unchanged. Counterfactual scenario [S4c]Depr:1955 was computed by fixing only the depreciation rate d_t to its 1955 level, leaving the rest of the model consistent with the full model.

F Online Appendix: sensitivity analyses

To assess the robustness of our findings, we conduct a series of tests focusing on our central result: the role of rising longevity in shaping wealth inequality. These tests explore whether the contribution of demographic factors is sensitive to alternative assumptions. We refer to the simulations presented in the main text as "primary", which include the baseline model and counterfactual scenarios. In this section, we add "alternative" simulations, where we modify aspects of the model and/or calibration. In these alternative simulations, we compare scenarios with longevity evolving according to the data (labeled "baseline" in figures and descriptions) to counterfactual scenarios where mortality rates are fixed at 1955 levels (referred to as '[S1]Longevity fixed at 1955').

Specifically, we explore several modifications to the model. First, we examine how variations in θ, the inverse elasticity of intertemporal substitution, impact our results. Second, we incorporated persistent differences in interest rates between individuals with a college education and those with less than a college education. Third, we excluded discount factor shocks to assess their relevance. Fourth, we applied an alternative specification for the income process. Fifth, we assume a higher path of technology growth. Finally, instead of assuming that bequests are distributed equally between all surviving agents in a cohort, we allow for an unequal distribution.

F.1 An alternative calibration: intertemporal elasticity of substitution

The value of θ in our baseline model reflects relatively low risk aversion and an intertemporal elasticity of substitution at the upper end of the estimates from microeconomic studies. Given the evolving nature of uncertainty over the analyzed period—particularly with rising income uncertainty—this parameter plays a significant role and could influence our comparison of demographic factors with the effects of income inequality on wealth inequality.

To address this concern, we modify the inverse elasticity of intertemporal substitution, θ, from 1.5 to 3. This parameter also governs relative risk aversion. To assess the robustness of our results, we analyze the contribution of demographic factors in the alternative scenario with $\theta = 3$, as shown in Figure F.1, and compare it with our primary scenario, shown in Figure 2, where $\theta = 1.5$.

The contribution of rising longevity to wealth inequality changes only slightly between the two scenarios. In 1975, it is 0.79 Gini points in the alternative scenario compared to 0.9 in the primary scenario. Similarly, in 2015, the contributions are nearly identical, with 1.41 Gini points in the alternative scenario and 1.4 in the primary. The difference becomes somewhat larger by 2050, where the contribution is 1.58 Gini points in the alternative scenario versus 1.45 in the primary.

Figure F.1: Baseline vs counterfactual scenario of constant longevity ($\theta = 3$)

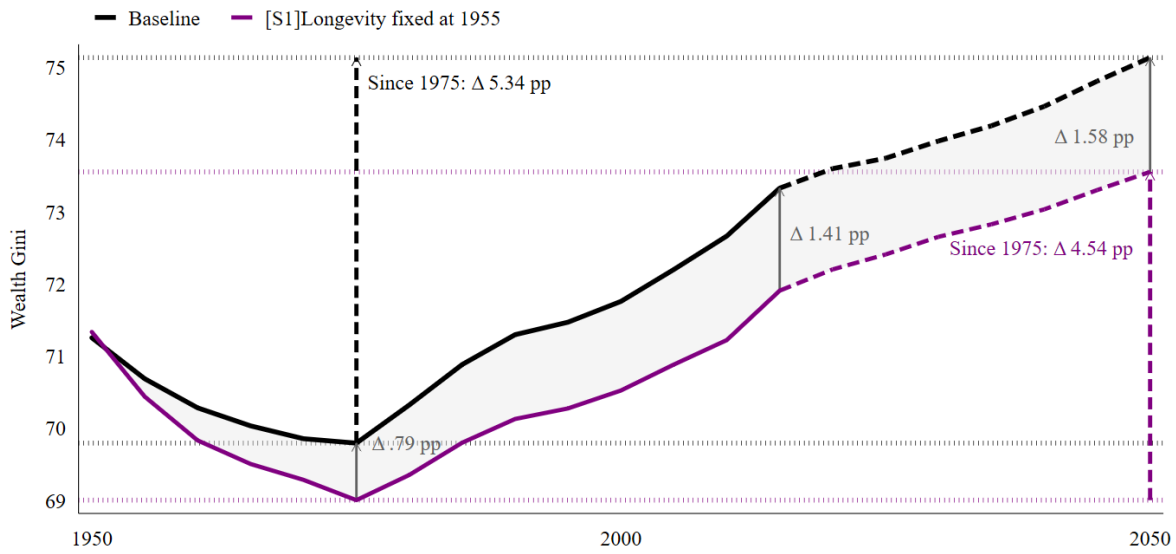

Note: The black line shows the level of the wealth Gini coefficient in the baseline model with $\theta = 3$. The violet line illustrates the wealth Gini coefficient from a counterfactual simulation where mortality rates, used both in calculating the population structure and in the consumer problem, are held constant at their 1955 levels, while all other aspects align with the baseline simulation.

With a higher value of relative risk aversion, the precautionary motive for saving strengthens, leading all agents to hold larger amounts of assets. As a result, the overall level of the Gini coefficient is lower and remains more stable over time compared to the primary calibration. Nevertheless, the role of longevity in shaping wealth inequality remains consistent with the results from the primary calibration.

F.2 Introducing heterogeneous rates of return

A large body of literature demonstrates that persistently heterogeneous asset returns are important contributors to wealth inequality (as discussed in the literature review in the Introduction section). Therefore, we conduct a robustness check incorporating heterogeneous rates of return based on education level s. Specifically, we assume that a gross after-tax return is $1 + \tilde{r}_{s,t} + \epsilon^r_{s,j,t}$, where $\tilde{r}_{s,t} = \underline{r}_t + x_s$. The difference in the deterministic parts of returns between the two education levels is a constant $x_H - x_L$ and we normalize $x_L = 0$. The endogenous variable $\underline{r}_t$ is such that the after-tax net capital income in the economy equals the net return on savings.

$$\tilde{r}_{t+1} K_{t+1} = \sum_{s \in \{L,H\}} \sum_{j=1}^{J} N_{s,j,t} \int_{\Omega} \tilde{r}_{s,t+1} a_{s,j+1,t+1}\left(z_{s,j,t}\right) d\mathbb{P}_{s,j,t}.$$

To calibrate this version of the model, we calculate the average value of x_H using SCF data from Kuhn et al. (2020b). The SCF dataset provides information on portfolio composition (three asset classes: equity and business wealth, real estate, and safe financial assets) at the household level. Following Bach et al. (2020), we use gross expected rates of return for these asset classes to calculate the expected rates of return on portfolios: the value-weighted CRSP index for equity, the Case-Shiller index for real estate, and the US one-month T-bill for safe financial assets. We proxy expected returns by average returns over the 1981 to 2016 period. We then calculate average portfolio returns by the education level of the household head.

Households with heads with college education have annual rates of return that are higher on average by 62 basis points, compared to households whose heads have less than college education. We convert the difference to 5-year periods to use as input to our model. The implied value of x_H equals 0.0365.

To assess the robustness of our results, similarly to the approach in the previous section, we analyze the contribution of demographic factors in this alternative scenario with persistent interest rate heterogeneity presented in Figure F.2, and compare it with our primary scenario, shown in Figure 2, which assumes no persistence in interest rate heterogeneity.

Introducing persistent heterogeneity in interest rates slightly increases the contribution of rising longevity to wealth inequality. In 1975, the contribution rises to 1.02 Gini points in the alternative scenario, compared to 0.9 in the primary. By 2015, the contribution increases to 1.56 Gini points in the alternative scenario and 1.4 in the primary, remaining close. By 2050, the contribution grows further to 1.57 Gini points in the alternative scenario, compared to 1.45 in the primary.

Figure F.2: Baseline vs counterfactual scenario of constant longevity (persistently heterogeneous rates of return)

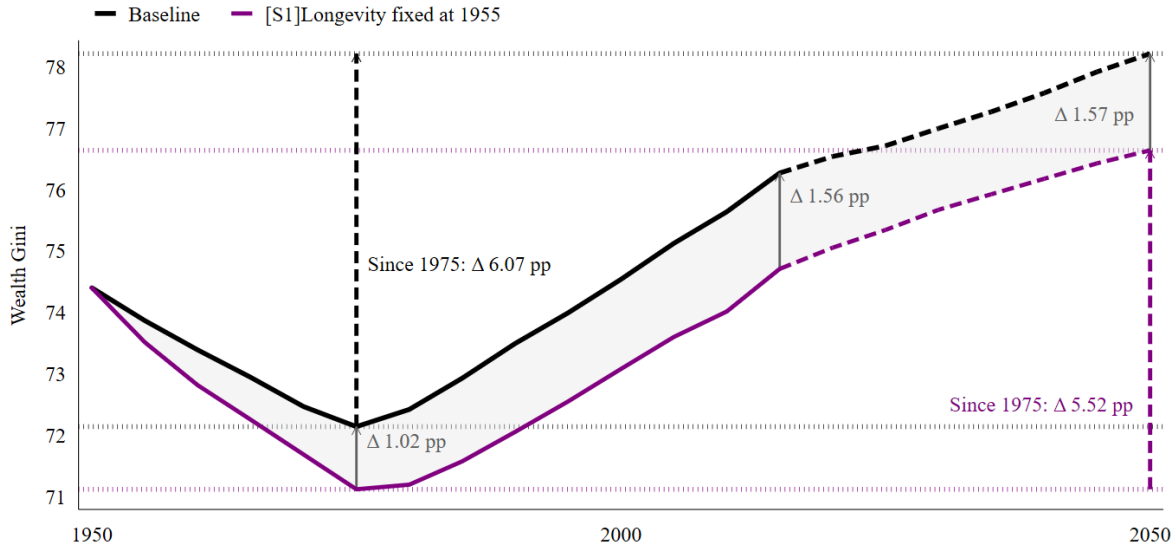

Note: The black line shows the level of the wealth Gini coefficient in the baseline model with heterogeneity in rates of return. The violet line illustrates the wealth Gini coefficient from a counterfactual simulation where mortality rates, used both in calculating the population structure and in the consumer problem, are held constant at their 1955 levels, while all other aspects align with the baseline simulation.

With heterogeneous rates of return, the overall Gini coefficient increases slightly, and the contribution of demographic factors to wealth inequality rises modestly as well. This occurs because higher returns for households with college education amplify the effects of rising longevity on wealth accumulation. Longer lifespans allow individuals with higher returns to accumulate more wealth over time, exacerbating inequality. Note also that households with college education experience a larger increase in longevity (see Figure B.2). While the effect is more pronounced in the long term, the interaction between rising longevity and return heterogeneity highlights how these factors together contribute to the growing concentration of wealth.

F.3 Model without discount factor shocks

Discount factor shocks increase asset dispersion among households that hold assets and serve as a significant source of uncertainty after retirement. They also improve the model's alignment with data on the share of households without accumulated wealth. By including these shocks, the model more accurately captures the *level* of wealth inequality, as they effectively represent various phenomena not explicitly modeled. However, the interaction between these shocks and the old-age saving motive in the context of rising longevity remains unclear.

To address this concern, we assume the absence of discount factor shocks. To implement this, we set $\delta_{s,j,t} = \bar{\delta}$ for all households and all periods. To examine the robustness of our findings, as in the previous two sections, we investigate the role of demographic factors in this alternative scenario, shown in Figure F.3, and compare it to the primary scenario depicted in Figure 2.

Figure F.3: Baseline vs counterfactual scenario of constant longevity (no discount factor shocks)

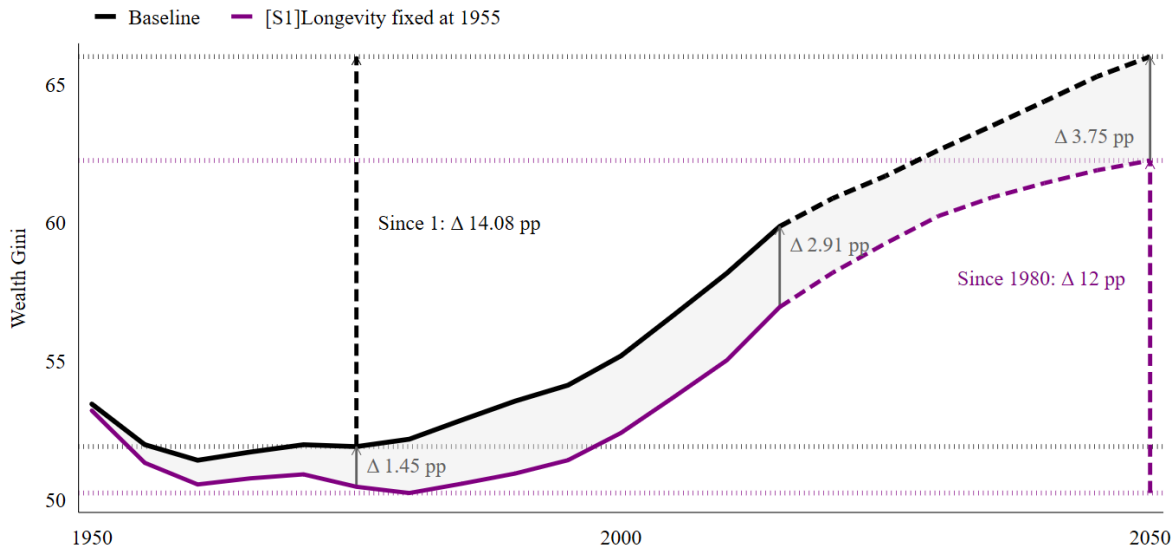

Note: The black line shows the level of the wealth Gini coefficient in the baseline model without discount factor shocks. The violet line illustrates the wealth Gini coefficient from a counterfactual simulation where mortality rates, used both in calculating the population structure and in the consumer problem, are held constant at their 1955 levels, while all other aspects align with the baseline simulation.

The model without discount factor shocks produces Gini coefficient levels lower than those observed in the data. Additionally, the decline in wealth inequality between 1950 and 1975 is much smaller than in the primary scenario.[19] However, the absence of discount factor shocks significantly amplifies the role of demographics in shaping wealth inequality. Without changes in longevity, the Gini coefficient is lower by 1.45 points in 1975, compared to less than 1 point in the primary calibration. Later, rising longevity contributes more prominently to rising wealth inequality, with their impact reaching 2.9 percentage points by 2015 and 3.75 points by 2050 (compared to approximately 1.5 points in the primary).

By removing discount factor shocks, an important source of heterogeneity is eliminated from the model, which affects the level of the wealth Gini coefficient. However, this adjustment does not alter our main conclusion regarding the contribution of demographic factors to wealth inequality. If

[19] This version of the model also generates almost no hand-to-mouth agents, in contrast to the more than 20% observed in the PSID data.

anything, it strengthens the argument for the critical role of rising longevity in shaping inequality trends.

F.4 An alternative calibration: income process without "superstars"

The calibration of "superstars" is controversial. In the literature, the authors sometimes use the "superstar" income state to match wealth inequality. Instead, we match the share of business income in total household income. This modeling choice can affect the implications of income inequality for wealth inequality in numerous ways, sometimes with the opposite directions.

To verify the role of this assumption for our key result, we consider an alternative calibration of the income process (3). This calibration excludes the separate "superstars" state. Instead, we estimate a standard five-state income process. Using PSID data, we jointly include salaried workers and individuals categorized as "superstars" in the entire sample to estimate the deterministic component $\zeta_{s,j}$ and the parameters of the process for the idiosyncratic component $\omega_{s,j,t}$. After discretizing the AR(1) process for $\omega_{s,j,t}$, we do not add the additional state corresponding to business income.

Compared to the primary calibration, this sensitivity analysis results in slightly more persistent idiosyncratic components for income processes: $\varrho_{\omega,L} = 0.982$ and $\varrho_{\omega,H} = 0.987$ (versus 0.980 and 0.985 in the primary calibration).

Figure F.4: Baseline vs counterfactual scenario of constant longevity (no "superstars")

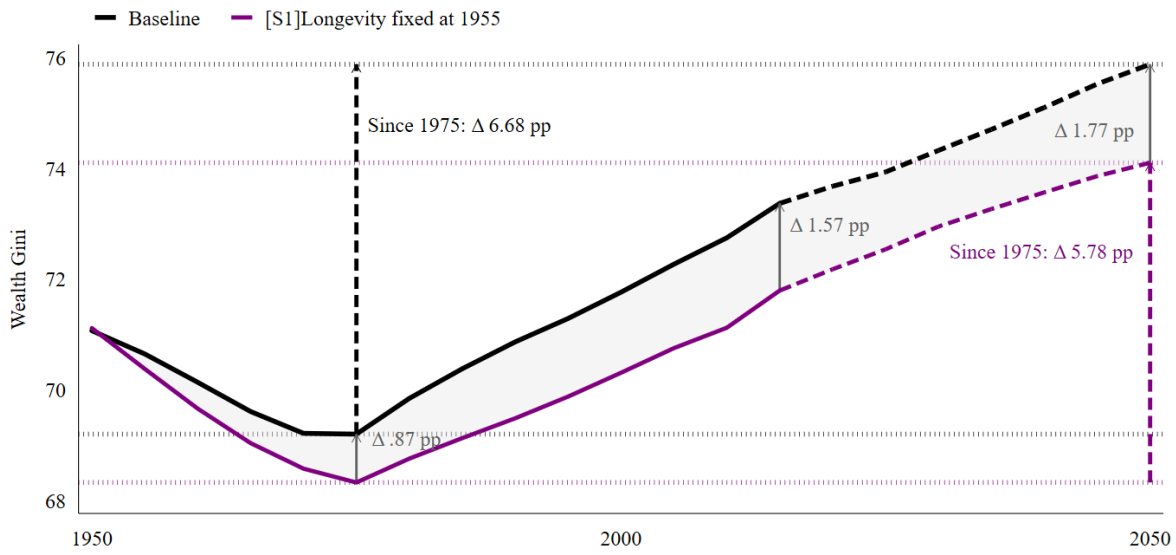

Note: The black line shows the level of the wealth Gini coefficient in the baseline model without the extra income state. The violet line illustrates the wealth Gini coefficient from a counterfactual simulation where mortality rates, used both in calculating the population structure and in the consumer problem, are held constant at their 1955 levels, while all other aspects align with the baseline simulation.

To evaluate the robustness of our findings, we follow the approach taken in the previous sections and analyze the role of demographic factors in this alternative scenario without "superstars," shown in Figure F.4, and compare it to the primary scenario with "superstars," depicted in Figure 2.

The model without "superstars" produces the wealth Gini coefficient levels that are lower than in the primary calibration. However, the absence of "superstars" slightly amplifies the role of demographic factors in shaping wealth inequality. Without changes in longevity, the Gini coefficient declines by 0.87 Gini points in 1975, compared to 0.9 in the primary calibration - almost identical. Later, however, rising longevity contributes more substantially to rising wealth inequality, with their

impact reaching 1.57 Gini points by 2015 and 1.77 points by 2050 (compared to approximately 1.5 points in the primary calibration).

In a model without "superstars", an important source of heterogeneity in our model, income inequality, becomes less pronounced. This shift lowers the contribution of within-cohort inequality to overall inequality, making the impact of between-cohort inequality more significant. Consequently, the argument for the critical role of rising longevity in driving inequality trends is further strengthened.

F.5 An alternative calibration: higher productivity growth rate

The debate about future evolution of TFP growth is unsettled. In the main text, we follow Fernald (2016). To study the sensitivity of our results to this assumption. We explore an alternative path of projected total factor productivity (TFP). This scenario could represent, for instance, the widespread adoption of AI (Brynjolfsson et al., 2021). Instead of assuming that the annual TFP growth rate stabilizes at 0.6% as in our primary scenario, we consider an alternative where the growth rate rebounds to over 1% annually. For this purpose, we use a projected path from the January 2025 vintage of the CBO Long-Term Economic Projections (Congressional Budget Office, 2025).

Note that due to differences in how the TFP is calculated in PWT 10 (our primary data source) and in the CBO's projections. These two measures are not directly comparable. For example, Shackleton (2013) reports that the average annual TFP growth rate in 1960-2010 in the U.S. was approximately 1.8%. The corresponding number in PWT 10 is 0.64%. We use the path from the CBO as an example of a higher trajectory, as shown in Figure F.5. The assumed terminal TFP growth rate is higher than in any period since the 1960s.

Figure F.5: Primary and alternative TFP growth rate

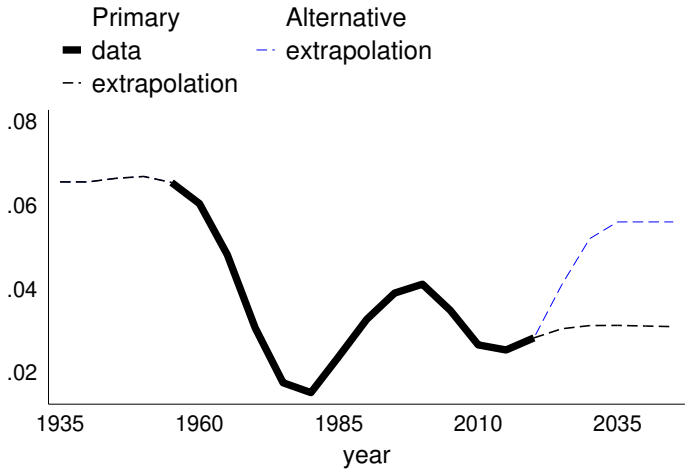

Note: Data are taken from Penn World Tables 10 (variable `rtfpna`). The data was adjusted to five-year periods. We also remove the cyclical component by applying Hodrick-Prescott filter. The values for each period are obtained as five-year averages of the trend component. The black dashed lines is the extrapolated path we use in the baseline calibration. The blue dashed line is the alternative projected path from Congressional Budget Office (2025) we use in the sensitivity check.

Again, to evaluate the robustness of our results, we examine the contribution of demographic factors in this alternative scenario, shown in Figure F.6, and compare it to the primary scenario depicted in Figure 2. Figure F.6 serves as a counterpart to Figure 2 in the main text.

The alternative projection of productivity growth somewhat lowers the contribution of rising

longevity to wealth inequality. In 1975, the contribution is 0.69 Gini points in the alternative scenario, compared to 0.9 in the primary. By 2015, the contribution increases to 1.02 Gini points in the alternative scenario versus 1.4 in the primary. By 2050, the contribution rises further to 1.08 Gini points in the alternative scenario, compared to 1.45 in the primary.

Steeper TFP growth contributes to an increase in wealth inequality. Between 1975 and 2050, the Gini coefficient grows by 5.83 points in the alternative scenario compared to 5.62 points in the primary. This result is consistent with findings that slower TFP growth reduces wealth inequality, as shown in Figure E.3.

TFP growth influences wealth inequality through multiple channels. Higher TFP growth leads to higher interest rates, which tend to amplify wealth inequality, although theoretically it is not impossible that they reduces it. TFP growth also affects the trajectory of income over the life cycle: with steeper income growth, individuals have less incentive to save early in life, and this effect is most likely particularly pronounced among low-income individuals, which tends to lead to increse in wealth inequality.

In general, higher projected TFP growth should increase wealth inequality, as it is in our simulations. Additionally, with faster income growth, old-age savings become a less important motive for asset accumulation. As a result, the contribution of demographic factors to wealth inequality diminishes under scenarios of higher TFP growth.

Qualitatively, the role of demographic factors in shaping wealth inequality remains consistent with our primary analysis. Quantitatively, however, its impact is somewhat smaller. Compared to the primary calibration, the effect of increased longevity is reduced by approximately 25%.

Figure F.6: Baseline vs counterfactual scenario of constant longevity (TFP growth rate)

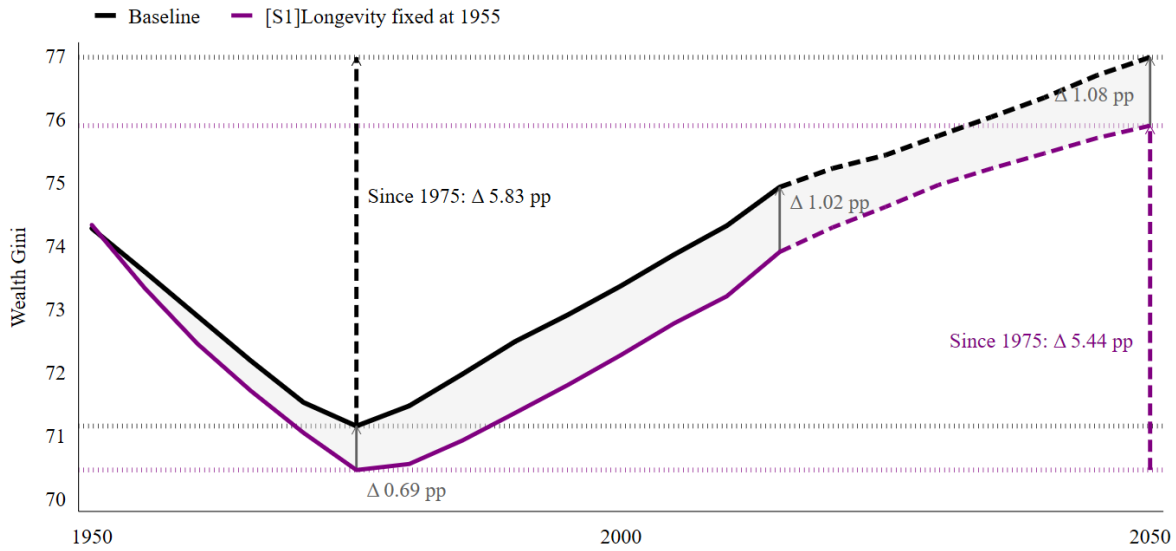

Note: The black line shows the level of the wealth Gini coefficient in the baseline model with alternative future TFP growth rate path. The violet line illustrates the wealth Gini coefficient from a counterfactual simulation where mortality rates, used both in calculating the population structure and in the consumer problem, are held constant at their 1955 levels, while all other aspects align with the baseline simulation.

F.6 An alternative calibration: unequal distribution of bequests

Halvorsen et al. (2024) analyze the wealth of the top 0.1% at age 50 in Norway and find that high initial wealth among top wealth owners accounts for approximately one-third of the wealth gap

between them and median households. In contrast, using the same data, Black et al. (2024) argue that bequests are almost irrelevant. The discrepancies between these studies, particularly due to differences in addressing the underreporting of inheritances, underscore the complexity of this issue.

The focus of our paper is on changes in wealth inequality within the "bottom 99%" in the U.S., specifically the roles of rising old-age longevity and income inequality in driving these changes. Evidence on the role of inheritances in the U.S. is mixed. For example, Hendricks (2001) report that while bequests are not evenly distributed—only 5% of households inherit more than 5% of lifetime earnings, and recipients of large bequests hold 2.5 times more wealth at retirement—inheritances explain only a small portion of this wealth gap. Approximately 50% of households in the top 1% of the wealth distribution in the SCF data did not receive any inheritance. Wolff (2002) and Wolff and Gittleman (2014) argue that bequests decrease wealth inequality in the SCF data, while Boserup et al. (2016) find that in Denmark, bequests reduce the top 1% wealth share but increase overall wealth inequality. Overall, the literature indicates that while bequests may significantly impact the top 1%, their influence on the "bottom 99%" appears limited and remains a topic of ongoing debate.

Given the ongoing debate in the literature, we examine whether an uneven distribution of bequests would affect our results. In the primary scenario, bequests are redistributed uniformly among individuals in the same cohort and with the same education level. In the alternative scenario, bequests are allocated to individuals with the same education level aged $j = 6$ (corresponding to ages 45–49). The distribution is as follows: 70% of individuals receive no bequests, 20% receive 50% of the total, and the remaining 10% receive the other 50%.

Following the approach from previous sections, we evaluate the robustness of our results by examining the contribution of demographic factors under this alternative scenario. The results are presented in Figure F.7 and compared to the primary scenario shown in Figure 2 in the main text. Figure F.7 serves as a direct counterpart to Figure 2.

Figure F.7: Baseline vs counterfactual scenario of constant longevity (unequal bequest distribution)

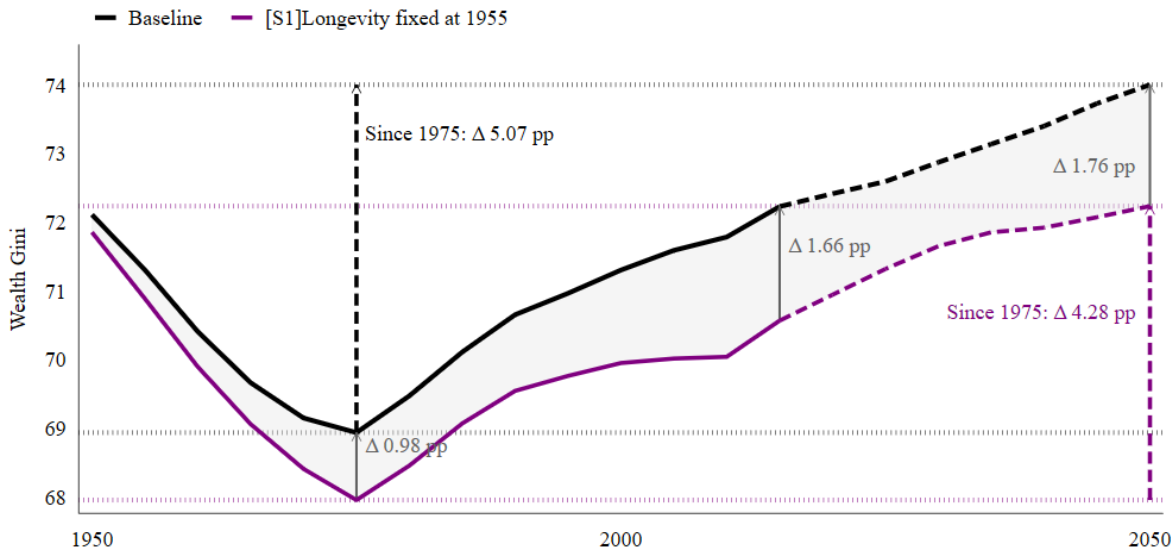

Note: The black line shows the level of the wealth Gini coefficient in the baseline model with an unequal distribution of bequests. The violet line illustrates the wealth Gini coefficient from a counterfactual simulation where mortality rates, used both in calculating the population structure and in the consumer problem, are held constant at their 1955 levels, while all other aspects align with the baseline simulation.

With the alternative bequest distribution the contribution of demographic factors to wealth

inequality becomes somewhat stronger. In 1975, the contribution is 0.98 Gini points in the alternative scenario, compared to 0.9 in the primary. By 2015, the contribution increases to 1.66 Gini points in the alternative scenario versus 1.4 in the primary. By 2050, the contribution rises further to 1.76 Gini points in the alternative scenario, compared to 1.45 in the primary.

These results indicate that with a more unequal distribution of bequests, the impact of demographic factors on wealth inequality becomes slightly more pronounced. This occurs because, with a low probability of receiving a bequest, individuals respond more strongly to increases in longevity. Consequently, the reinforcing effect of demographic transitions on inequality is amplified.

References

Alvaredo, F., Garbinti, B., and Piketty, T. (2017). On the share of inheritance in aggregate wealth: Europe and the usa, 1900–2010. *Economica*, 84(334):239–260.

Autor, D., Goldin, C., and Katz, L. F. (2020). Extending the race between education and technology. *AEA Papers and Proceedings*, 110:347–51.

Bach, L., Calvet, L. E., and Sodini, P. (2020). Rich pickings? risk, return, and skill in household wealth. *American Economic Review*, 110(9):2703–47.

Barro, R. J. and Sahasakul, C. (1983). Measuring the Average Marginal Tax Rate from the Individual Income Tax. *The Journal of Business*, 56(4):419–452.

Bauluz, L. and Meyer, T. (2024). The wealth of generations. WID Working Paper 2024/04, WID - World Inequality Lab.

Black, S. E., Devereux, P. J., Landaud, F., and Salvanes, K. G. (2024). The (un)importance of inheritance. *Journal of the European Economic Association*.

Boppart, T. and Krusell, P. (2020). Labor supply in the past, present, and future: A balanced-growth perspective. *Journal of Political Economy*, 128(1):118–157.

Boserup, S. H., Kopczuk, W., and Kreiner, C. T. (2016). The role of bequests in shaping wealth inequality: Evidence from danish wealth records. *American Economic Review*, 106(5):656–61.

Brynjolfsson, E., Rock, D., and Syverson, C. (2021). The productivity j-curve: How intangibles complement general purpose technologies. *American Economic Journal: Macroeconomics*, 13(1):333–72.

Case, A. and Deaton, A. (2021). Life expectancy in adulthood is falling for those without a ba degree, but as educational gaps have widened, racial gaps have narrowed. *Proceedings of the National Academy of Sciences*, 118(11):e2024777118.

Chetty, R., Stepner, M., Abraham, S., Lin, S., Scuderi, B., Turner, N., Bergeron, A., and Cutler, D. (2016). The association between income and life expectancy in the United States, 2001-2014. *Journal of American Medical Association*, 315(16):1750–1766.

Congressional Budget Office (2025). The budget and economic outlook.

Deaton, A. and Paxson, C. (2000). Growth and saving among individuals and households. *Review of Economics and Statistics*, 82(2):212–225.

Fernald, J. G. (2016). Reassessing Longer-Run U.S. Growth: How Low? Working Paper Series 2016-18, Federal Reserve Bank of San Francisco.

Ferrere, A. and Navarro, G. (2018). The Heterogeneous Effects of Government Spending : It's All About Taxes. International Finance Discussion Papers 1237, Board of Governors of the Federal Reserve System (U.S.).

Goldin, C. and Katz, L. F. (2008). *The Race Between Education and Technology.* Belknap Press for Harvard University Press.

Gomez, M. (2023). Decomposing the Growth of Top Wealth Shares. *Econometrica*, 91(3):979–1024.

Guvenen, F. (2009). An empirical investigation of labor income processes. *Review of Economic Dynamics*, 12(1):58–79.

Halvorsen, E., Hubmer, J., Ozkan, S., and Salgado, S. (2024). Why Are the Wealthiest So Wealthy? New Longitudinal Empirical Evidence and Implications for Theories of Wealth Inequality. Working Papers 2024-013, Federal Reserve Bank of St. Louis.

Hendricks, L. (2001). Bequests and retirement wealth in the united states. Technical report.

Hubmer, J., Krusell, P., and Smith., A. A. (2021). Sources of us wealth inequality: Past, present, and future. *NBER Macroeconomics Annual*, 35:391–455.

Kuhn, M., Schularick, M., and Steins, U. I. (2020a). Income and wealth inequality in America, 1949–2016. *Journal of Political Economy*, 128(9):3469–3519.

Kuhn, M., Schularick, M., and Steins, U. I. (2020b). Income and wealth inequality in America, 1949–2016. *Journal of Political Economy*, 128(9):3469–3519.

Lewandowski, M., Makarski, K., Svejnar, J., and Tyrowicz, J. (2024). Factors behind rising U.S. wealth inequality: a decomposition and policy implications. GRAPE Working Paper 100, GRAPE.

McDaniel, C. (2007). Average tax rates on consumption, investment, labor and capital in the oecd: 1950-2003. *mimeo*.

McGrattan, E. and Prescott, E. (2017). On financing retirement with an aging population. *Quantitative Economics*, 8(1):75–115.

Mertens, K. and Montiel Olea, J. L. (2018). Marginal tax rates and income: New time series evidence. *The Quarterly Journal of Economics*, 133(4):1803–1884.

Nishiyama, S. and Smetters, K. (2007). Does social security privatization produce efficiency gains? *The Quarterly Journal of Economics*, 122(4):1677–1719.

Piketty, T. and Saez, E. (2003). Income Inequality in the United States, 1913–1998*. *The Quarterly Journal of Economics*, 118(1):1–41.

Shackleton, R. (2013). Total factor productivity growth in historical perspective. Technical report.

Straub, L. (2019). Consumption, savings, and the distribution of permanent income.

Wolff, E. and Gittleman, M. (2014). Inheritances and the distribution of wealth or whatever happened to the great inheritance boom? *The Journal of Economic Inequality*, 12(4):439–468.

Wolff, E. N. (2002). Inheritances and wealth inequality, 1989-1998. *American Economic Review*, 92(2):260–264.